C.P. No. 516
(19,522)
A.R.C. Technical Report

C.P. No. 516
(19,522)
A.R.C. Technical Report

MINISTRY OF AVIATION

AERONAUTICAL RESEARCH COUNCIL

CURRENT PAPERS

An Approximate Method for Calculating the Laminar Boundary Layer on an Infinite Swept Wing with Arbitrary Velocity and Suction Distribution

By

A. W. Lindfield and H. G. Pinsent

LONDON: HER MAJESTY'S STATIONERY OFFICE

1960

PRICE 5s 6d NET

C.P. No. 516

H.P. Research Report No.37

July, 1957

An Approximate Method for Calculating the Laminar Boundary Layer on an Infinite Swept Wing with Arbitrary Velocity and Suction Distributions

- By -

A. W. Lindfield and H. G. Pinsent

SUMMARY

This report is concerned with the calculation of the crossflow velocity profiles in the laminar boundary layer on an infinite swept wing.

A brief survey, of the early attempts to solve the problem, is given first.

In our early work we tried to obtain the crossflow by calculating the chordwise and spanwise solutions. The chordwise solution was first attempted with a method due to Truckenbrodt. This failed, and eventually the chordwise solution was obtained with a method due to Dr. Head, which gave good accuracy. The spanwise solution was solved by an extension of a method due to Sinha.

It was soon found that although these solutions were of good accuracy in themselves, in the region we were considering their small errors combined to give as much as 50-100% error in the crossflow.

It was then realised that the crossflow must be determined directly. An equation was obtained for it, which also depended on the chordwise solution. Dr. Head's method gives the chordwise solution to sufficient accuracy for this purpose.

The method of solution finally adopted was to form a difference equation for the crossflow and determine the increments in the crossflow across a chordwise step. The accuracy obtained by this approach was quite reasonable, as shown by comparison with Pfenninger's exact solution.

The method uses graphical differentiation to solve the partial differential difference equation for the crossflow, and is able to cope with discontinuities in velocity gradient or suction distribution. Only one approximation is used in this method and this enables the solution to proceed at reasonably large steps.

The solution was started at 30% chord, since no difficulty was anticipated at stagnation, and also as the region of immediate interest was just before and after the beginning of suction.

However, we later found that at stagnation the method broke down, since the crossflow changed rapidly and the approximation used was not good enough. A better approximation was substituted, the equation slightly rearranged, and the method changed to one of integration. This gave reasonable results, but the process was very slow. Once away from the high leading-edge crossflow, the differential method could be used again.

One purpose of the method is to obtain the crossflow accurately enough for its stability to be determined. This may be done by means of a

criterion/

criterion which relates the second derivative of the profile at the wall to an inflectional Reynolds number based on the distance of the inflection point from the wall and the velocity at the inflection point of the profile. An extended treatment is given in the section dealing with stability.

The crossflow profiles obtained are good enough to measure the above stability parameters.

Also of interest is the determination of the suction distribution required to stabilise the flow over an infinite swept wing having a given pressure distribution.

In the Appendix an alternative solution of the stagnation problem is given which proves to be a more rapid method.

CONTENTS

Introduction/

Introduction

The critical value of Owen's crossflow Reynolds number (125) which was established for the stagnation zone of a swept wing created the impression that full-chord laminar flow over a swept wing would lead to uneconomically large suction quantities. Thus it appeared that application of boundary layer control to stabilize a laminar flow would be restricted to straight wings of relatively low critical Mach number.

It is to the credit of the American research group under Dr. Pfenninger[5] to have shown by exact calculations that the Owen criterion had not a unique value for the whole chord of the wing. They showed that its critical value depended not only on the thickness of the boundary layer and the peak value of the crossflow velocity but also on the shape of the crossflow velocity profiles. Moreover they could show that the flow could be stabilized in an adverse pressure gradient with moderate suction quantities.

Pfenninger obtained exact solutions of the boundary-layer equations by extensive computation with an IBM high-speed digital computor.

Taking the same wing and sweep as Pfenninger, and the same pressure distribution and suction distribution (A_1 case) we developed an approximate method for obtaining the crossflow profiles, which needed nothing more complicated than a desk machine for computation.

We are grateful for having these exact solutions available to use as a yardstick, as we feel that progress would have been slow without them, and a critical assessment of the accuracy of the results would have been impossible.

Notation

c = chord in flight direction

$\bar{c}$ = chord perpendicular to leading edge (chordwise direction)

$2D^*$ = dissipation term in the energy equation of Head's method

$$= 2\int_0^{\delta/\theta} \left(\frac{\theta}{U}\right)^2 \left(\frac{\partial u}{\partial z}\right)^2 d\left(\frac{z}{\theta}\right)$$

H = ratio of displacement thickness to momentum thickness = δ^*/θ

H_ε = ratio of energy thickness to momentum thickness = ε/θ

$$K = W_o \bigg/ \left(\frac{d\bar{U}}{dX}\right)^{\frac{1}{2}}$$

ℓ = profile parameter used in Head's method = $\dfrac{\theta}{U}\left(\dfrac{\partial u}{\partial z}\right)_o = t^{*\frac{1}{2}}\left(\dfrac{\partial T}{\partial Z}\right)_o$

$$L = \frac{dW_o}{dX}\left(\frac{d\bar{U}}{dX}\right)^{\frac{1}{2}} \bigg/ \frac{d^2\bar{U}}{dX^2}$$

m = profile parameter used in Head's method = $\dfrac{\theta^2}{U}\left(\dfrac{\partial^2 u}{\partial z^2}\right)_o = t^*\left(\dfrac{\partial^2 T}{\partial Z^2}\right)_o$

n/

n = crossflow velocity in boundary layer = $\dfrac{U_o \bar{U} \tan \Gamma}{(\bar{U}^2 + \tan^2 \Gamma)^{\frac{1}{2}}} \left(\dfrac{v}{V_o} - \dfrac{u}{U} \right)$

N = $\dfrac{v}{V_o} - \dfrac{u}{U} = S - T$

Rc = flight Reynolds number = $\dfrac{U_\infty c}{\nu}$

R$\bar{c}$ = chordwise Reynolds number = $\dfrac{U_o \bar{c}}{\nu}$

S = $\dfrac{v}{V_o}$

T = $\dfrac{u}{U}$

t* = $\left(\dfrac{\theta}{c} \right)^2 R_c = \left(\dfrac{\theta}{\bar{c}} \right)^2 R_{\bar{c}}$

U_∞ = flight velocity

U_o = chordwise component of flight velocity = $U_\infty \cos \Gamma$

U = local chordwise outer flow velocity

$\bar{U}$ = U/U_o

u = chordwise velocity in boundary layer

V_o = spanwise component of flight velocity = $U_\infty \sin \Gamma$

v = spanwise velocity in boundary layer

W = $R_c^{\frac{1}{2}} w/U_\infty$

w = vertical velocity in boundary layer

x = distance round surface in chordwise direction

X = $x/\bar{c}$

X* = $\ln \left(\dfrac{d\bar{U}}{dX} \right)$

z = distance vertical to surface

Z = $R_c^{\frac{1}{2}} \; z/c$

Z* = $Z \left(\dfrac{d\bar{U}}{dX} \right)^{\frac{1}{2}}$

β = angle between chordwise direction and outer flow streamline direction

Γ = angle of sweep

δ/

δ = boundary layer thickness

δ^* = chordwise displacement thickness $= \int_0^\infty (1 - T)\, dz$

ε = chordwise energy thickness $= \int_0^\infty T\,(1 - T^2)\, dz$

θ = chordwise momentum thickness $= \int_0^\infty T(1 - T)\, dz$

$$\lambda = - \frac{\theta w_o}{\nu} = - t^{*\frac{1}{2}} W_o$$

$$\Lambda = \frac{\theta^2}{\nu} \frac{dU}{dx} = t^* \frac{d\bar{U}}{dX}$$

ν = coefficient of kinematic viscosity.

Suffix 'o' denotes values of a quantity taken at the surface, i.e., $Z = 0$

Suffix '1' denotes values of a quantity taken at the beginning of a step

Suffix '2' denotes values of a quantity taken at the end of a step.

1. The Crossflow

The crossflow is the component of flow in the boundary layer, which is parallel to the body surface and normal to the outer flow streamline. It has an important influence on the stability of the boundary layer.

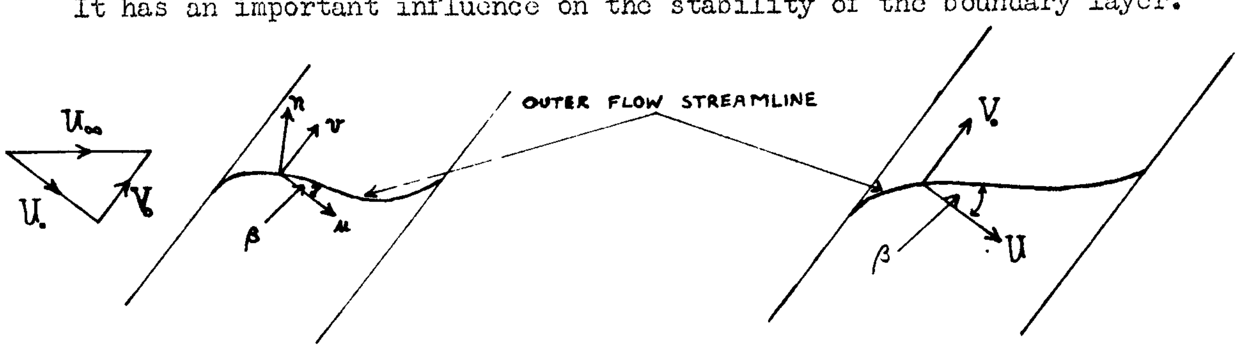

Fig.(i) Flow in the boundary layer.

Fig.(ii) Flow at the edge of the boundary layer.

From Fig.(i)

$$n = v \cos\beta - u \sin\beta = \frac{v}{V_o} V_o \cos\beta - \frac{u}{U} U \sin\beta$$

From Fig.(ii)

$$U \sin\beta = V_o \cos\beta = \frac{U\, V_o}{(U^2 + V_o^2)^{\frac{1}{2}}}$$

$$\therefore n = \frac{U\, V_o}{(U^2 + V_o^2)^{\frac{1}{2}}} \left(\frac{v}{V_o} - \frac{u}{U} \right) = \frac{U_o\, \bar{U} \tan\Gamma}{(\bar{U}^2 + \tan^2\Gamma)^{\frac{1}{2}}} \left(\frac{v}{V_o} - \frac{u}{U} \right)$$

2. First Attempts at Solution

For an infinite wing, the boundary layer equations may be separated into (a) an independent chordwise equation and (b) a spanwise equation, which depends on the chordwise solution.

Since the crossfloq is proportional to $\left(\frac{v}{V_o} - \frac{u}{U} \right)$ it seemed reasonable in our early work to evaluate u/U then v/V_o and hence obtain n.

2.1 The chordwise solution

2.1.1 Truckenbrodt's method

Of the various methods available, a method due to Truckenbrodt[1], was decided on, since it could be used equally well in regions with or without suction. Since the method gave us no means of determining a velocity profile, Thwaites' cubic profile was used.

Agreement was fair over the non-suction region. However, when the method was extended into the sucked region with adverse pressure gradient, it broke down since it predicted separation at about 83% chord, which from Pfenninger's results did not occur. It was clear that the method was unable to give reliable results in the presence of an adverse pressure gradient.

2.1.2 Extension of Truckenbrodt's method

It was decided to extend the curves in Truckenbrodt's work so as to cope with high suctions and adverse pressure gradients. This work was nearing completion, when Dr. Head drew our attention to the method which he had developed. Work on the extension of Truckenbrodt's method was stopped and Dr. Head's method adopted.

2.1.3 The method due to Dr. Head

This is a two parameter system, using the momentum and energy integral equations[2]. The method is accurate, giving momentum thickness to within about 1 or 2% and giving excellent velocity profiles on comparison with Pfenninger's exact solutions (Figs.1 and 2). This was true even in the adverse pressure gradient region. If necessary the accuracy could be further improved by reconstructing the working charts with greater precision.

2.2 The spanwise solution

At first, in conjunction with the Truckenbrodt method for the chordwise flow, the spanwise flow was determined by a method due to Rott and Crabtree[3], but this method could only be used for zero suction. Again a Thwaites' cubic velocity profile was taken. The crossflow profile obtained in this manner was poor, and no boundary layer thickness was given due to the 'cut off' effect of the cubic profiles (Fig.3).

2.2.1 Sinha's method

Dr. Head drew our attention to Sinha's Ph.D thesis[4], in which a method of solving the spanwise boundary layer momentum equation, using the one-parameter Schlichting profiles was described. The method was found to give reasonable results in the non-sucked region. However, the crossflow profiles were about 20% in error when compared with the Pfenninger solution (Fig.4). This one-parameter method was unable to cope with a discontinuous change in velocity gradient or suction distribution.

It/

It was decided to extend Sinha's method to a two-parameter system and use a spanwise energy equation as well as the momentum equation. The method thus became somewhat like Head's chordwise method.

The Schlichting profiles were still used to evaluate the functions needed to produce the charts required. To obtain velocity profiles, it was assumed that they were two parameters, of the type used by Head in the chordwise flow and therefore given by his charts. By this method, good results were obtained through the discontinuities and the spanwise velocity profiles when checked with Pfenninger's solution were reasonably correct.

It was found that there was some tendency in the suction region for the spanwise profiles of Pfenninger's solution to be of a different type to those of his chordwise solution (Fig.5).

The crossflow profiles when compared with Pfenninger's were found to be very much in error (Fig.6). It was realised that the present approach in the regions being considered was inadequate since the small errors in the u/U and v/V_0 profiles were sufficient to make the error of their difference of the same magnitude as the crossflow itself.

With this in mind, a method was developed which would give the crossflow directly.

In the Appendix, it will be shown that we can use the earlier approach near stagnation.

3. Present Method of Solution

It was originally thought that it would not be practically possible to use the method of calculating chordwise and spanwise solutions to obtain the crossflow. In the Appendix, the latest work shows that this method might be used from stagnation since the magnitude of N is about 0.2 and the errors are acceptable on this value. These errors could be considerably reduced by increasing the accuracy of Head's charts.

3.1 The crossflow equation

3.1.1 Derivation of the crossflow equation

The boundary layer equations for an infinite wing are:-

Chordwise $$u \frac{\partial u}{\partial x} + w \frac{\partial u}{\partial z} = U \frac{dU}{dx} + \nu \frac{\partial^2 u}{\partial z^2} \qquad \ldots (1)$$

Spanwise $$u \frac{\partial v}{\partial x} + w \frac{\partial v}{\partial z} = \nu \frac{\partial^2 v}{\partial z^2} \qquad \ldots (2)$$

Continuity $$\frac{\partial u}{\partial x} + \frac{\partial w}{\partial z} = 0 \qquad \ldots (3)$$

Making these equations non-dimensional we obtain

Chordwise $$\bar{U}T \frac{\partial T}{\partial X} + W \frac{\partial T}{\partial Z} = (1 - T^2) \frac{d\bar{U}}{dX} + \frac{\partial^2 T}{\partial Z^2} \qquad \ldots (1a)$$

Spanwise $$\bar{U}T \frac{\partial S}{\partial X} + W \frac{\partial S}{\partial Z} = \frac{\partial^2 S}{\partial Z^2} \qquad \ldots (2a)$$

Continuity $$\frac{\partial (\bar{U}T)}{\partial X} + \frac{\partial W}{\partial Z} = 0 \qquad \ldots (3a)$$

where $T = u/U$ $S = v/V_0$.

Subtracting equation (1a) from (2a) and writing $N = S - T$ we obtain

$$\bar{U}T \frac{\partial N}{\partial X} + W \frac{\partial N}{\partial Z} = \frac{\partial^2 N}{\partial Z^2} - (1 - T^2) \frac{d\bar{U}}{dX} \qquad \ldots (4)$$

Equation (4) is termed the 'N-equation'. N is the quantity we wish to determine, since the crossflow n at any chordwise station is proportional to N.

The/

The N-equation itself could be used in a step-by-step process, in which one could obtain an approximate N from an extrapolated $\partial N/\partial X$. A better approximation for $\partial N/\partial X$ could then be obtained by substituting N back in the N-equation. It was found, however, that it was more accurate to calculate the increment in N (i.e., ΔN) for a step and add this to the N at the beginning of the step, since a large error on ΔN would in general be an acceptable error on N.

A difference equation was therefore derived from the N-equation.

3.1.2 The difference equation

If we denote a step in X by ΔX, and denote values at the beginning of the step by a suffix '1' and values at the end of a step by a suffix '2', then we can write down the two equations

$$\bar{U}_2 T_2 \left(\frac{\partial N}{\partial X} \right)_2 + W_2 \frac{\partial N_2}{\partial Z} = \frac{\partial^2 N_2}{\partial Z^2} - (1 - T_2^2)\left(\frac{d\bar{U}}{dX} \right)_2 \qquad \ldots (4a)$$

and

$$\bar{U}_1 T_1 \left(\frac{\partial N}{\partial X} \right)_1 + W_1 \frac{\partial N_1}{\partial Z} = \frac{\partial^2 N_1}{\partial Z^2} - (1 - T_1^2)\left(\frac{d\bar{U}}{dX} \right)_1 \qquad \ldots (4b)$$

Now subtract (4b) from (4a) and writing

$$\Delta N = N_2 - N_1 \qquad \Delta \left(\frac{\partial N}{\partial X} \right) = \left(\frac{\partial N}{\partial X} \right)_2 - \left(\frac{\partial N}{\partial X} \right)_1$$

$$\Delta (\bar{U}T) = \bar{U}_2 T_2 - \bar{U}_1 T_1 \qquad \Delta W = W_2 - W_1$$

$$\Delta \left[(1 - T^2) \frac{d\bar{U}}{dX} \right] = (1 - T_2^2) \left(\frac{d\bar{U}}{dX} \right)_2 - (1 - T_1^2) \left(\frac{d\bar{U}}{dX} \right)_1$$

we have

$$\bar{U}_2^2 T_2 \Delta \left(\frac{\partial N}{\partial X} \right) + \Delta(\bar{U}T) \left(\frac{\partial N}{\partial X} \right)_1 + W_2 \frac{\partial \Delta N}{\partial Z} + \Delta W \frac{\partial N_1}{\partial Z} = \frac{\partial^2 \Delta N}{\partial Z^2} - \Delta \left[(1-T^2) \frac{d\bar{U}}{dX} \right] \qquad \ldots (4c)$$

which becomes after rearrangement,

$$\Delta \left(\frac{\partial N}{\partial X} \right) = \frac{1}{\bar{U}_2 T_2} \left\{ \frac{\partial^2 \Delta N}{\partial Z^2} - W_2 \frac{\partial \Delta N}{\partial Z} - \Delta W \frac{\partial N_1}{\partial Z} - \Delta(\bar{U}T)\left(\frac{\partial N}{\partial X} \right)_1 - \Delta \left[(1-T^2) \frac{d\bar{U}}{dX} \right] \right\} \qquad (5)$$

This is the equation used to evaluate the crossflow. It should be noted that it is ex[illegible] .

3.1.3 The boundary conditions

It has been found useful to consider both equation (4) and equation (4c) evaluated at the boundary, i.e., $Z = 0$.

The following boundary conditions have been used.

(i) From equation (4)

$$\left.\begin{aligned}
\left(\frac{\partial^2 N}{\partial Z^2}\right)_o &= W_o\left(\frac{\partial N}{\partial Z}\right)_o + \frac{d\bar{U}}{dX} \\
\left(\frac{\partial^3 N}{\partial Z^3}\right)_o &= W_o\left(\frac{\partial^2 N}{\partial Z^2}\right)_o \\
\left(\frac{\partial^4 N}{\partial Z^4}\right)_o &= W_o\left(\frac{\partial^3 N}{\partial Z^3}\right)_o - \frac{\partial}{\partial X}\left(\frac{\bar{U}\ell}{t^{*\frac{1}{2}}}\right)\left(\frac{\partial N}{\partial Z}\right)_o + \frac{2\bar{U}\ell}{t^{*\frac{1}{2}}}\left[\frac{\partial}{\partial z}\left(\frac{\partial N}{\partial X}\right)\right]_o - \frac{2\ell^2}{t^*}\frac{d\bar{U}}{dX}
\end{aligned}\right\} \quad \text{.. (6)}$$

(ii) From equation (4c)

$$\left.\begin{aligned}
\left(\frac{\partial^2 \Delta N}{\partial Z^2}\right)_o &= (W_2)_o\left(\frac{\partial \Delta N}{\partial Z}\right)_o + (\Delta W)_o\left(\frac{\partial N_1}{\partial Z}\right)_o + \Delta\left(\frac{d\bar{U}}{dX}\right) \\
\left(\frac{\partial^3 \Delta N}{\partial Z^3}\right)_o &= (W_2)_o\left(\frac{\partial^2 \Delta N}{\partial Z^2}\right)_o + (\Delta W)_o\left(\frac{\partial^2 N_1}{\partial Z^2}\right)_o \\
\left(\frac{\partial^4 \Delta H}{\partial Z^4}\right)_o &= (W_2)_o\left(\frac{\partial^3 \Delta N}{\partial Z^3}\right)_o + (\Delta W)_o\left(\frac{\partial^3 N_1}{\partial Z^3}\right)_o + \frac{2\bar{U}_2\ell_2}{t_2^{*\frac{1}{2}}}\left[\frac{\partial}{\partial z}\Delta\left(\frac{\partial N}{\partial X}\right)\right]_o + 2\Delta\left(\frac{\bar{U}\ell}{t^{*\frac{1}{2}}}\right) \\
&\quad \times\left[\frac{\partial}{\partial Z}\left(\frac{\partial N}{\partial X}\right)_1\right]_o - \left[\frac{\partial}{\partial X}\left(\frac{\bar{U}\ell}{t^{*\frac{1}{2}}}\right)\right]_2\left(\frac{\partial \Delta N}{\partial Z}\right)_o - \Delta\left[\frac{\partial}{\partial X}\left(\frac{\bar{U}\ell}{t^{*\frac{1}{2}}}\right)\right]\left(\frac{\partial N_1}{\partial Z}\right)_o - 2\Delta\left(\frac{\ell^2}{t^*}\frac{d\bar{U}}{dX}\right)
\end{aligned}\right\} \quad \text{(7)}$$

For zero suction $(W_2)_o = 0$ and $(\Delta W)_o = 0$.

3.2 Solution of the crossflow equation

3.2.1 Preliminaries

To obtain the chordwise solution, $\bar{U}$ and $d\bar{U}/dX$ will have already been determined.

For the crossflow solution, it will be necessary to determine over the whole chord, the functions

$$T,\ W,\ \text{and also}\ \ \bar{U}T\ \ \text{and}\ \ (1 - T^2)\frac{d\bar{U}}{dX}$$

T is determined directly by the use of Head's charts and W is determined from the continuity equation.

$$\text{Thus}\quad W = W_o - \int_o^z \frac{\partial}{\partial X}(\bar{U}T)\, dZ \qquad \text{... (8)}$$

Plots of T and W versus X with Z as parameter are required so that these functions may be determined with reasonable accuracy at any value of X required.

3.2.2 Using the method

Writing equation (5) again

$$\Delta\left(\frac{\partial N}{\partial X}\right) = \frac{1}{\bar{U}_2 T_2}\left\{\frac{\partial^2 \Delta N}{\partial Z^2} - W_2\frac{\partial \Delta N}{\partial Z} - \Delta W\frac{\partial N_1}{\partial Z} - \Delta(\bar{U}T)\left(\frac{\partial N}{\partial X}\right)_1 - \Delta\left[(1-T^2)\frac{d\bar{U}}{dX}\right]\right\} \qquad \text{... (5)}$$

The/

The object of the method is to evaluate everything on the R.H.S. of (5) and hence we are able to obtain the increment to $\partial N/\partial X$ across the step, and thus the increment in N.

The problem of starting from stagnation conditions will be dealt with later, so for the present section, it will be assumed that we know

$N = N_1$, $\dfrac{\partial N}{\partial Z} = \dfrac{\partial N_1}{\partial Z}$ and $\dfrac{\partial N}{\partial X} = \left(\dfrac{\partial N}{\partial X}\right)_1$ at the beginning of a step.

We also know $\bar{U}_2$ T_2, W_2, ΔW, $\Delta(UT)$ and $\Delta\left[(1-T^2)\dfrac{d\bar{U}}{dX}\right]$. Thus everything is known except $\dfrac{\partial \Delta N}{\partial Z}$ and $\dfrac{\partial^2 \Delta N}{\partial Z^2}$.

We now make an approximation for ΔN on the R.H.S. of equation (5). The approximation taken was

$$\Delta N = \left(\frac{\partial N}{\partial X}\right)_{\text{extrapolated}} \Delta X \qquad \ldots (9)$$

$\left(\dfrac{\partial N}{\partial X}\right)_{\text{extrap.}}$ was obtained from a running plot of $\dfrac{\partial N}{\partial X}$ versus X with Z as parameter. We were able to write $\dfrac{\partial \Delta N}{\partial Z} = \dfrac{\partial}{\partial Z}\left(\dfrac{\partial N}{\partial X}\right)_{\text{extrap.}} \Delta X.$

$\dfrac{\partial}{\partial Z}\left(\dfrac{\partial N}{\partial X}\right)_{\text{extrap.}}$ was plotted and smoothed and thus $\dfrac{\partial^2}{\partial Z^2}\left(\dfrac{\partial N}{\partial X}\right)_{\text{extrap.}}$ was obtained. This was also plotted and smoothed. The differentiations were carried out graphically. On multiplying by ΔX we obtain $\dfrac{\partial \Delta N}{\partial Z}$ and $\dfrac{\partial^2 \Delta N}{\partial Z^2}$.

In order to draw the graphs of these derivatives near $Z = 0$, the boundary conditions of (7) were used.

Thus for zero-suction, $\dfrac{\partial^2 \Delta N}{\partial Z^2} = \Delta\left(\dfrac{d\bar{U}}{dX}\right)$ and so the starting slope of the graph of $\dfrac{\partial \Delta N}{\partial Z}$ is known and thus the curve may be drawn in the best position. Similarly for the graph of $\dfrac{\partial^2 \Delta N}{\partial Z^2}$ we have a starting slope of zero.

If there is suction, then the best combination of wall derivatives must be taken to satisfy the boundary conditions and the plotted points for $\dfrac{\partial \Delta N}{\partial Z}$ and $\dfrac{\partial^2 \Delta N}{\partial Z^2}$. Where necessary it was considered to be more important to satisfy the boundary conditions than to follow the points of $\dfrac{\partial \Delta N}{\partial Z}$ and $\dfrac{\partial^2 \Delta N}{\partial Z^2}$ near $Z = 0$.

If a running plot of $\frac{\partial N}{\partial X}$ versus X for each Z is kept (Fig.7) it is a simple matter to compute ΔN and hence N. It was found sufficient to calculate the ΔN from the trapezium rule but alternatively it might be determined more accurately by integration. To proceed to the next step, a new starting value of $\frac{\partial N}{\partial Z}$ will be required.

This/

This will in fact be $\partial N_2/\partial Z$.

Thus $$\frac{\partial N_2}{\partial Z} = \frac{\partial N_1}{\partial Z} + \Delta\left(\frac{\partial N}{\partial Z}\right) \doteqdot \frac{\partial N_1}{\partial Z} + \frac{\partial \Delta N}{\partial Z} \qquad \ldots (10)$$

Since we were interested in the region of suction with an adverse pressure gradient, we started the solution at 30% chord. As suction started at 63% chord, the method had a good trial in regions of non-suction and suction. The results of the calculations are given in Figs.8, 9 and 10.

3.2.3 Discontinuities in suction or velocity gradient

These could be dealt with by fairing the curves so that no discontinuity occurred. However, since the object was to compare calculated results with Pfenninger's exact solutions, it was decided to accept the discontinuities. The results proved to be quite satisfactory, although the discontinuity in $\partial N/\partial X$ was infinite.

3.2.4 Size of step

From the running plots of $\partial N/\partial X$ versus X, one can decide on the step size.

If the $\partial N/\partial X$ plots have a large curvature then a small step size must be used, so that the approximation $\Delta N = \left(\frac{\partial N}{\partial X}\right)_{extrap.} \Delta X$ is a reasonable one for the step.

If the $\partial N/\partial X$ plots are nearly linear then quite large steps can be made. It should be noted that the step size does <u>not</u> depend on the shape of the curves of T, W, $\bar{U}T$ or $(1 - T^2)\frac{d\bar{U}}{dX}$.

It is now realised that an unnecessary number of steps were taken in the non-sucked region and that the work from X = 0.3 to X = 0.6311 could have been completed in about 5 steps. In the sucked region, when the calculation had reached X = 0.65, it was decided to try some large steps, and the calculation was taken to X = 0.90 with steps at X = 0.65, 0.67, 0.7, 0.8, 0.9. Thus two steps of 10% were tried.

As can be seen from the results (Fig.10) the original calculated points at X = 0.7, 0.8 and 0.9 are in error at the peak of the crossflow profile and at the tail end. It can be seen (Fig.11) that this is due to the sudden change in shape of the $\partial N/\partial X$ plots and therefore the approximation

$$\Delta N = \left(\frac{\partial N}{\partial X}\right)_{extrap.} \Delta X$$ breaks down.

We decided to try and converge these results. Mean curves of N were drawn through the circle points, and derivatives with respect to Z obtained graphically. The N-equation (4) was then used to obtain a new $\partial N/\partial X$. A mean $\partial N/\partial X$ was taken between the original calculated $\partial N/\partial X$ and the new one (this mean is shown in Fig.12) and ΔN computed from it. This converged the peaks (Fig.10 - crosses) but the tail ends were unaltered.

This tail end effect was found to be due to the chordwise solution being inaccurate there. This was partly because of the need for more accurate charts, but mainly because it was found to be difficult to read off values accurately from Head's charts in this part of the chordwise calculation.

4./

4. Starting at Stagnation

We now consider how to start at stagnation. We will consider first the more general case with suction.

4.1 The chordwise solution

The chordwise solution may be obtained with the use of Head's charts.

To obtain the stagnation values of ℓ, m, we have to solve the equation - (obtained from the momentum and energy equations)

$$\ell + 2m + (2\ell - 1)2D^* - 3(m + \ell^2)H_\varepsilon + (m + \ell \times 2D^*)H = 0 \quad \dots (11)$$

where for this 2 parameter system $2D^*$, H, H_ε are functions of ℓ and m.

This has been solved approximately for suction cases.

The suction parameter is given by

$$\lambda = \frac{\ell + m(H + 2)}{\ell(H + 2) - 1} \quad \dots (12)$$

while the boundary condition is

$$\frac{1}{W_o^2}\frac{d\bar{U}}{dX} = \frac{-(m + \ell\lambda)}{\lambda^2} \quad \dots (13)$$

We define $K = W_o \Big/ \left(\frac{d\bar{U}}{dX}\right)^{\frac{1}{2}}$ and $L = \frac{dW_o}{dX}\left(\frac{d\bar{U}}{dX}\right)^{\frac{1}{2}} \Big/ \frac{d^2\bar{U}}{dX^2}$.

Therefore the boundary condition is $\frac{1}{K^2} = -\frac{(m + \ell\lambda)}{\lambda^2}$ ... (13a)

The stagnation curve of ℓ and m is a single line, therefore all quantities, i.e., λ, H, H_ε, $2D^*$, m. Λ and K can be defined entirely in terms of ℓ.

Thus, once the parameter K is known, ℓ is known and thus the whole stagnation solution is known (Figs.13, 14 and 15). The velocity profile is determined from Head's charts.

We will still require starting values of $t^{*\prime} = \frac{dt^*}{dX}$ and $H_\varepsilon' = \frac{dH_\varepsilon}{dX}$. First we determine ℓ' and m'. These are given as the solution of the linear equations.

$$[2\lambda + (\ell+\lambda)K^2 + (5+2H)\lambda^2 - \Lambda(2\lambda + \ell K^2)H_\ell]\ell' + [(5+2H)\lambda + K^2 - \Lambda(2\lambda + \ell K^2)H_m]m'$$
$$= [\{(2+H)\ell - 1\}(K^2 - 2KL) - \ell KL - \lambda]\Lambda \frac{d^2\bar{U}}{dX^2}\Big/\frac{d\bar{U}}{dX} \quad .. (14)$$

and/

and

$$[\{\ell-\lambda-\Lambda(H-2)\}(2\lambda+\ell K^2)H_{\varepsilon_\ell}+(1-\Lambda H_\ell)(2\lambda+\ell K^3)H_\varepsilon+\lambda\{2\lambda(H-1)H_\varepsilon+(H_\varepsilon-1)K^2\}-(2\lambda+\ell K^2)2D^*_o]\ell'$$

$$+[\{\ell-\lambda-\Lambda(H-2)\}(2\lambda+\ell K^2)H_{\varepsilon_m}-\Lambda(2\lambda+\ell K^3)H_\varepsilon H_m+2\lambda(H-1)H_\varepsilon+(H_\varepsilon-1)K^2-(2\lambda+\ell K^2)2D^*_m]m'$$

$$= [\ell(H-1)H_\varepsilon-(H_\varepsilon-1)](K^2-2KL)\Lambda \frac{d^2\bar{U}}{dX^2}\Big/\frac{d\bar{U}}{dX} \quad .. (15)$$

where $H_{\varepsilon_\ell} = \dfrac{\partial H_\varepsilon}{\partial \ell}$, $H_{\varepsilon_m} = \dfrac{\partial H_\varepsilon}{\partial m}$ and similarly for H and 2D* and these can all be obtained from Head's charts. Then

$$H'_\varepsilon = H_{\varepsilon_\ell}\,\ell' + H_{\varepsilon_m}\,m' \quad ... (16)$$

and

$$t^{*\prime} = \frac{-2\lambda(m'+\lambda\ell')}{(2\lambda+\ell K^2)\dfrac{d\bar{U}}{dX}} - \frac{2\Lambda(\lambda+\ell KL)}{2\lambda+\ell K^2}\,\frac{d^2\bar{U}}{dX^2}\Big/\left(\frac{d\bar{U}}{dX}\right)^2 \quad ... (17)$$

The starting value of t^* is given by $t^* = \Lambda\Big/\left(\dfrac{d\bar{U}}{dX}\right) = \dfrac{\lambda^2}{W_o^2}$ ... (18)

Starting values of H_ε, H and 2D* are readily obtained from Head's charts.

For zero suction, we have from the charts

$\ell = 0.3674$ $\quad m = -0.0876$ $\quad H_\varepsilon = 1.6368$ $\quad 2D^* = 0.4301$

$H = 2.1946$ $\quad \ell' = 0.01787 \dfrac{d^2\bar{U}}{dX^2}\Big/\dfrac{d\bar{U}}{dX}$ $\quad m' = -0.0138 \dfrac{d^2\bar{U}}{dX^2}\Big/\dfrac{d\bar{U}}{dX}$

$t^{*\prime} = -0.07379 \dfrac{\dfrac{d^2\bar{U}}{dX^2}}{\left(\dfrac{d\bar{U}}{dX}\right)^2}$ $\quad H'_\varepsilon = 0.0066 \dfrac{d^2\bar{U}}{dX^2}\Big/\dfrac{d\bar{U}}{dX}$ $\quad t^* = \dfrac{0.0876}{\dfrac{d\bar{U}}{dX}}$

4.2 The crossflow solution

The chordwise and N-equations are

$$\bar{U}T\frac{\partial T}{\partial X} + W\frac{\partial T}{\partial Z} = (1-T^2)\frac{d\bar{U}}{dX} + \frac{\partial^2 T}{\partial Z^2} \quad ... (1a)$$

and

$$\bar{U}T\frac{\partial N}{\partial X} + W\frac{\partial N}{\partial Z} = -(1-T^2)\frac{d\bar{U}}{dX} + \frac{\partial^2 N}{\partial Z^2} \quad ... (4)$$

and the continuity equation is

$$\frac{\partial(\bar{U}T)}{\partial X}\Big/$$

$$\frac{\partial(\bar{U}T)}{\partial X} + \frac{\partial W}{\partial Z} = 0 \quad \text{i.e.,} \quad W = W_o - \int_o^z \frac{\partial(\bar{U}T)}{\partial X}\, dZ \qquad \ldots (3a)$$

At stagnation $\bar{U} = 0$.

If we consider equations (1a) and (4) at stagnation, together with the continuity equation, we obtain after making the transformation

$$Z^* = Z\left(\frac{d\bar{U}}{dX}\right)^{\frac{1}{2}}$$

$$\frac{d^2T}{dZ^{*2}} + \left(\int_o^{z^*} TdZ^* - K\right)\frac{dT}{dZ^*} + (1 - T^2) = 0 \qquad \ldots (19)$$

and

$$\frac{d^2N}{dZ^{*2}} + \left(\int_o^{z^*} TdZ^* - K\right)\frac{dN}{dZ^*} - (1 - T^2) = 0 \qquad \ldots (20)$$

Further, if we differentiate equations (1a) and (4) with respect to X and then take stagnation conditions, we obtain, using the transformations

$$\left.\begin{aligned} X^* &= \ell n\left(\frac{d\bar{U}}{dX}\right) \\ Z^* &= Z\left(\frac{d\bar{U}}{dX}\right)^{\frac{1}{2}} \end{aligned}\right\} \qquad \ldots. (21)$$

$$\frac{d^2}{dZ^{*2}}\left(\frac{\partial T}{\partial X^*}\right) + \left[\int_o^{z^*} TdZ^* - K\right]\frac{d}{dZ^*}\left(\frac{\partial T}{\partial X^*}\right) - 3T\frac{\partial T}{\partial X^*} + 2\frac{dT}{dZ^*}\left[\int_o^{z^*}\frac{\partial T}{\partial X^*}\, dZ^*\right]$$

$$= \left[L - \tfrac{1}{2}K + \tfrac{1}{2}\int_o^{z^*} TdZ^*\right]\frac{dT}{dZ^*} \qquad .. (22)$$

and

$$\frac{d^2}{dZ^{*2}}\left(\frac{\partial N}{\partial X^*}\right) + \left[\int_o^{z^*} TdZ^* - K\right]\frac{d}{dZ^*}\left(\frac{\partial N}{\partial X^*}\right) - T\frac{\partial N}{\partial X^*}$$

$$= -2T\frac{\partial T}{\partial X^*} + \left[L - \tfrac{1}{2}K + \int_o^{z^*}\left(\tfrac{1}{2}T - 2\frac{\partial T}{\partial X^*}\right)dZ^*\right]\frac{dN}{dZ^*} \qquad \ldots (23)$$

where $K = W_o \Big/ \left(\frac{d\bar{U}}{dX}\right)^{\frac{1}{2}}$ and $L = \frac{dW_o}{dX}\left(\frac{d\bar{U}}{dX}\right)^{\frac{1}{2}} \Big/ \frac{d^2\bar{U}}{dX^2}$ as before.

With zero suction and suction gradient at stagnation, the equations (19), (20), (22) and (23) become independent of K and L, and so may be solved once and for all.

The first two have already been solved by other workers, e.g., the chordwise equation is effectively the stagnation Falkner-Skan equation.

We have approximately solved the equations for $\partial T/\partial X^*$ and $\partial N/\partial X^*$ by graphical and numerical methods for the case with $K = 0$ and $L = 0$.

5. Continuing the Solution away from Stagnation

(For the alternative method now being used, see Appendix).

The differential method broke down in the stagnation region since $\partial N/\partial X$ was changing too rapidly for the approximation taken for ΔN to be valid.

The difference equation (5) may be re-written as

$$\frac{\partial^2 \Delta N}{\partial Z^2} - W_2 \frac{\partial \Delta N}{\partial Z} - \Delta W \left(\frac{\partial N}{\partial Z} \right)_1 = \Delta \left[(1 - T^2) \frac{d\bar{U}}{dX} \right] + \Delta \left(\bar{U}T \frac{\partial N}{\partial X} \right) \quad \ldots (24)$$

We now make the following approximation for ΔN

$$\Delta N = \left\{ k \left(\frac{\partial N}{\partial X} \right)_1 + (1 - k) \left(\frac{\partial N}{\partial X} \right)_2 \right\} \Delta X$$

$$= \left\{ \left(\frac{\partial N}{\partial X} \right)_2 - k\Delta \left(\frac{\partial N}{\partial X} \right) \right\} \Delta X \quad \ldots (25)$$

Where k is a constant introduced to give consistency between the boundary condition from equation (24), i.e.,

$$\left(\frac{\partial^2 \Delta N}{\partial Z^2} \right)_0 = \Delta \left(\frac{d\bar{U}}{dX} \right) \quad \ldots (26)$$

and that obtained after differentiating the N-equation with respect to X.

The boundary condition for the differentiated N-equation is

$$\left[\frac{\partial^2}{\partial Z^2} \left(\frac{\partial N}{\partial X} \right) \right]_0 = \frac{d^2 \bar{U}}{dX^2} \quad \ldots (27)$$

From equation (25) we have

$$\left(\frac{\partial^2 \Delta N}{\partial Z^2} \right)_0 = \left\{ k \left[\frac{\partial^2}{\partial Z^2} \left(\frac{\partial N}{\partial X} \right)_1 \right]_0 + (1 - k) \left[\frac{\partial^2}{\partial Z^2} \left(\frac{\partial N}{\partial X} \right)_2 \right]_0 \right\} \Delta X$$

Substituting this in equation (26) and using equation (27) we have

$$k \left(\frac{d^2 \bar{U}}{dX^2} \right)_1 + (1 - k) \left(\frac{d^2 \bar{U}}{dX^2} \right)_2 = \frac{\Delta \left(\frac{\partial \bar{U}}{dX} \right)}{\Delta X}$$

i.e.,

$$\left(\frac{d^2 \bar{U}}{dX^2} \right)_2 - k\Delta \left(\frac{d^2 \bar{U}}{dX^2} \right) = \frac{\Delta \left(\frac{d\bar{U}}{dX} \right)}{\Delta X}$$

$$\therefore \quad k = \frac{\left(\frac{d^2 \bar{U}}{dX^2} \right)_2 - \frac{\Delta \left(\frac{d\bar{U}}{dX} \right)}{\Delta X}}{\Delta \left(\frac{d^2 \bar{U}}{dX^2} \right)} \quad \ldots (28)$$

(For/

(For the case where the curve of $d\bar{U}/dX$ varies linearly $k = \frac{1}{2}$).

Substituting ΔN into equation (24) we obtain an equation for $\left(\frac{\partial N}{\partial X}\right)_2$

$$\frac{\partial^2}{\partial Z^2}\left(\frac{\partial N}{\partial X}\right)_2 - W_2\frac{\partial}{\partial Z}\left(\frac{\partial N}{\partial X}\right)_2 - \frac{\bar{U}_2 T_2}{(1-k)\Delta X}\left(\frac{\partial N}{\partial X}\right)_2 = \frac{-k}{1-k}\left\{\frac{\partial^2}{\partial Z^2}\left(\frac{\partial N}{\partial X}\right)_1 - W_2\frac{\partial}{\partial Z}\left(\frac{\partial N}{\partial X}\right)_1\right\}$$

$$+ \frac{1}{(1-k)\Delta X}\left\{\Delta W\left(\frac{\partial N}{\partial Z}\right)_1 + \Delta\left[(1-T^2)\frac{d\bar{U}}{dX}\right] - \bar{U}_1 T_1\left(\frac{\partial N}{\partial X}\right)_1\right\} \qquad \ldots (29)$$

Equation (29) is solved by a graphical step-by-step method. An approximate determination of $\frac{\partial^2}{\partial Z^2}\left(\frac{\partial N}{\partial X}\right)_2$ is made and hence we obtain approximations to $\frac{\partial}{\partial Z}\left(\frac{\partial N}{\partial X}\right)_2$ and $\left(\frac{\partial N}{\partial X}\right)_2$. Putting these back into equation (29) we obtain an better approximation to $\frac{\partial^2}{\partial Z^2}\left(\frac{\partial N}{\partial X}\right)_2$ and thus proceed step-by-step until complete consistency is obtained between the integrating and computing processes.

The constants of integration are chosen so that

$$\left(\frac{\partial N}{\partial X}\right)_2 = 0 \text{ at } Z = 0 \text{ and } \left(\frac{\partial N}{\partial X}\right)_2 \to 0 \text{ as } Z \to \infty .$$

It is not possible to ensure that $\frac{\partial}{\partial Z}\left(\frac{\partial N}{\partial X}\right)_2 \to 0$ as $Z \to \infty$ except by altering the curve for $\frac{\partial^2}{\partial Z^2}\left(\frac{\partial N}{\partial X}\right)_2$ at the outer edge. Using this process, the solution is helped to converge more quickly. A comparison obtained by this process is given in Fig.16.

6. Determination of Stability

Professor Owen first suggested the Reynolds number based on the peak crossflow velocity and the thickness of the crossflow profile as a criterion for the magnitude of the crossflow. This Reynolds number was denoted by χ. It was found that for flow in the vicinity of a leading edge, the laminar boundary layer broke down if the value of this criterion exceeded a certain value (about 125) and this was accepted as a critical value. In the well known example of the rotating disc the critical value of χ was observed to be higher (about 330).

Pfenninger, in extensive calculations of crossflow profiles and their stability in regions of favourable and adverse pressure gradients and both with and without suction, showed that the critical value of χ depended to a marked degree on the shape of the crossflow profile and adopted the value of $\left[\frac{\partial^2 (n/n_{max})}{\partial (z/\delta)^2}\right]_o$ as a shape parameter.

Gregory/

Gregory found that if one plotted χ_{crit} against the second derivative, a roughly linear relationship was possible.

Latterly Owen has suggested a critical Reynolds number based on the distance of the inflection point from the wall, and the velocity at the inflection point of the profile (Fig.17). This has the advantage of reducing the range of variation of χ_{crit} considerably.

Thus for a profile to be stable, we require that the inflection Reynolds number should be less than the critical value corresponding to the second derivative of the profile at the wall.

The problem of determining a suction distribution to give stable laminar flow for a given chordwise pressure distribution may be solved by the use of the above criterion. The stability parameters would be obtained from the crossflow profile and the first boundary condition of the N-equation. The chordwise and crossflow solutions would proceed together.

7. Conclusions

It has been seen that the method due to Dr. Head for solving the chordwise laminar boundary layer gives excellent results over the full chord, coping with discontinuities in velocity gradient and suction.

The method of Sinha for solving the spanwise flow also gives reasonable results, while the extension of the method enables discontinuities to be overcome.

The differential method of solving the crossflow gives accurate results and can be quite rapid since steps of 5% chord may be taken over a considerable part of the wing.

In the vicinity of stagnation, it was found that the crossflow could be given with reasonable accuracy by calculating the spanwise and chordwise solutions separately. This accuracy could be increased by making improvements to the working charts of Head's method.

In nearly all cases, the comparison of the velocity profiles with Pfenningers exact solution was quite favourable, the crossflow profiles being obtained accurately enough for their stability parameters to be determined.

It is felt that the method provides a simple and reasonably accurate way of calculating the laminar boundary layer for an infinite swept wing.

Acknowledgements

This work was carried out under the direction of Dr. G. V. Lachmann, Director of Research, Handley Page Ltd. The authors would like to express their gratitude to Mr. J. B. Edwards of the Research Department, Handley Page Ltd., Professor Owen of Manchester University and Dr. M. R. Head of Cambridge University who have frequently offered valuable advice; and also to the assistance given by Miss P. A. Lock, Research Department, Handley Page Ltd.

References/

References

No.	Author(s)	Title, etc.
1	Truckenbrodt	Inst. für Strömungsmechanik, T. H. Braunschweig. Rep. No.55/6a.
2	Head, M. R.	An unpublished report dealing with the solution of the two-dimensional laminar boundary layer equation.
3	Rott, N. and Crabtree, L. F.	Simplified laminar boundary layer calculations for bodies of revolution and for yawed wings. Journal of the Aeronautical Sciences - August, 1952.
4	Sinha, K. D. P.	Ph.D. Thesis dealing with the solution of the spanwise laminar boundary layer equation.
5	Pfenninger, W. Raetz, G. S. and Brown, W. B.	Note on design problems of swept laminar suction wings. Northrop Aircraft Inc. Report No.NAI-55-549. BLC-79.

APPENDIX/

APPENDIX

Recent Alternative Method Used to Obtain The Profiles Near Stagnation

Since the method used in Section 5 was very slow, it was desirable to find a quick way of calculating the crossflow in the vicinity of stagnation.

On consideration, it was realised that in the original calculations of the crossflow, where it was determined from the difference of spanwise and chordwise velocity profiles, we were trying to obtain differences of the order of 0.06 and getting errors of about ± 0.025.

At stagnation, however, we require differences of about 0.20, and since these differences are large we felt that there would be a possibility of the method used in the original calculations succeeding. We also found that for the spanwise solution the stagnation condition given by Sinha was incorrect, making the spanwise boundary layer, in our earlier work, too thick.

With this condition corrected, the spanwise solution was calculated from stagnation back to 30% chord. In this region there is no suction and the Blasius profile may be taken as a good approximation for the spanwise profile.

Profiles of $N = \frac{v}{V_o} - \frac{u}{U}$ were calculated at a number of stations and compared with Pfenninger's exact solutions. These are shown in Figs.18 and 19. It will be seen that agreement is reasonable even back to 30% chord. The approximate solution could be bettered if the accuracy of Head's charts were increased.

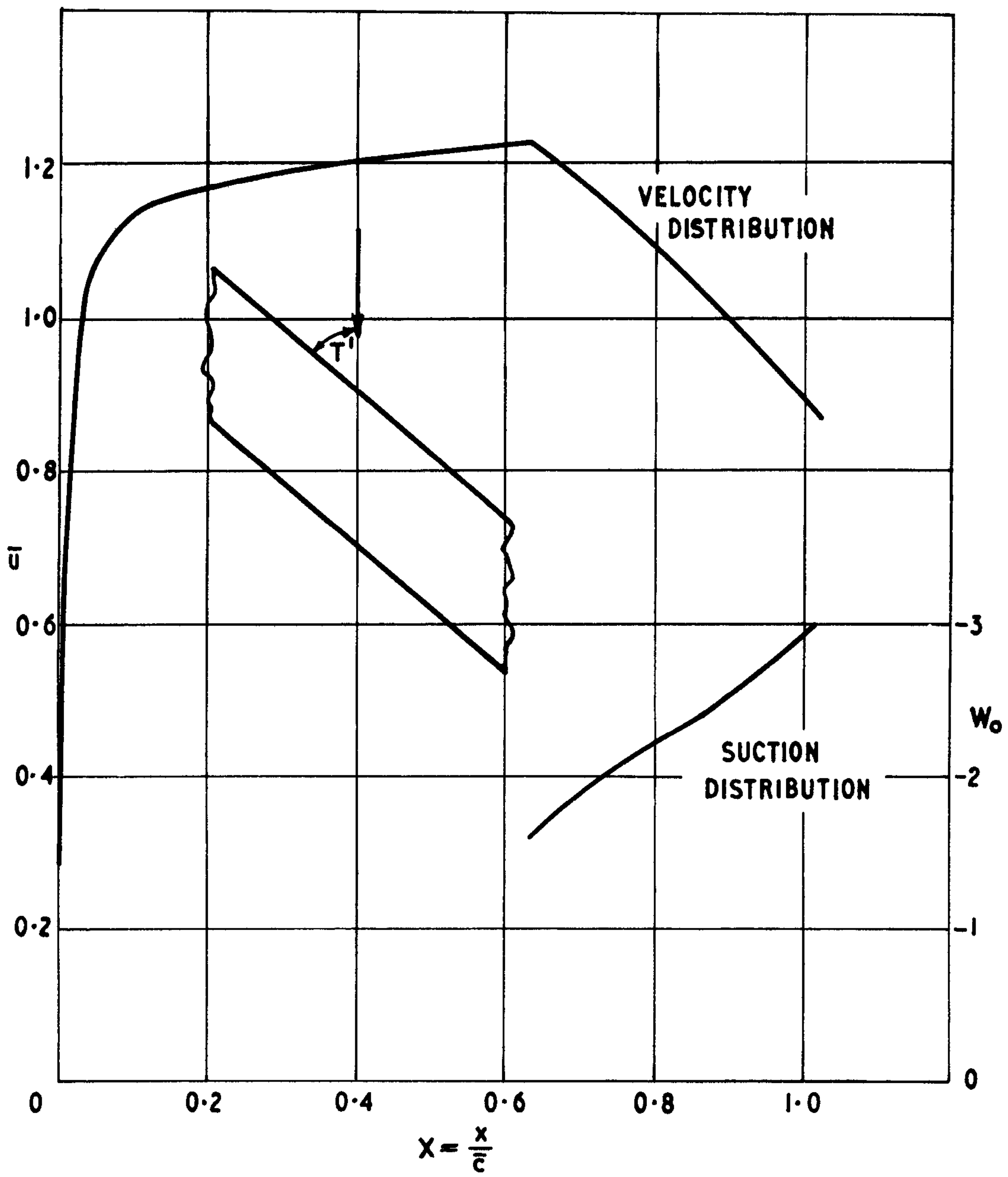

FIG.1. VELOCITY AND SUCTION DISTRIBUTION

M

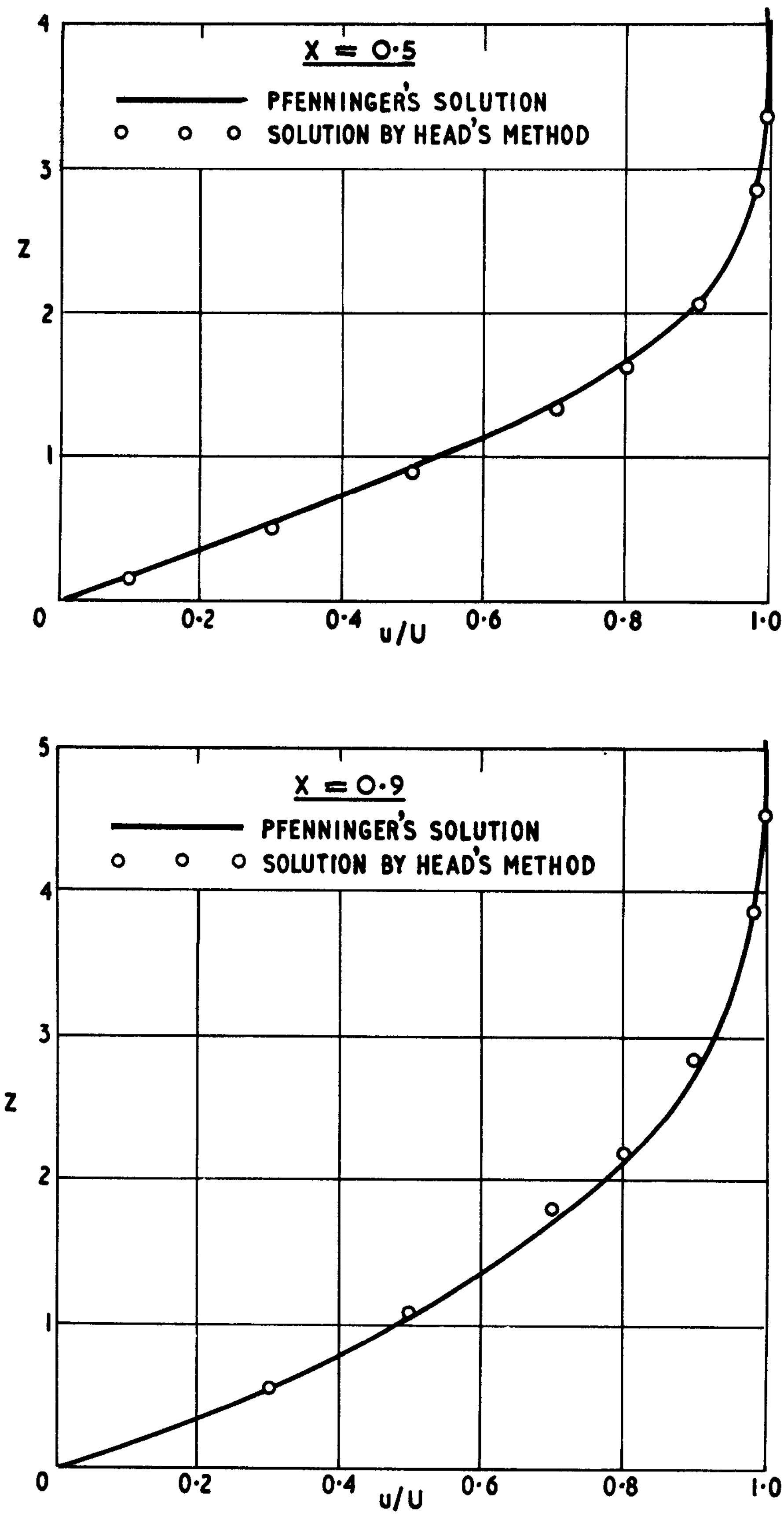

FIG. 2. CHORDWISE SOLUTION

E.E.M.

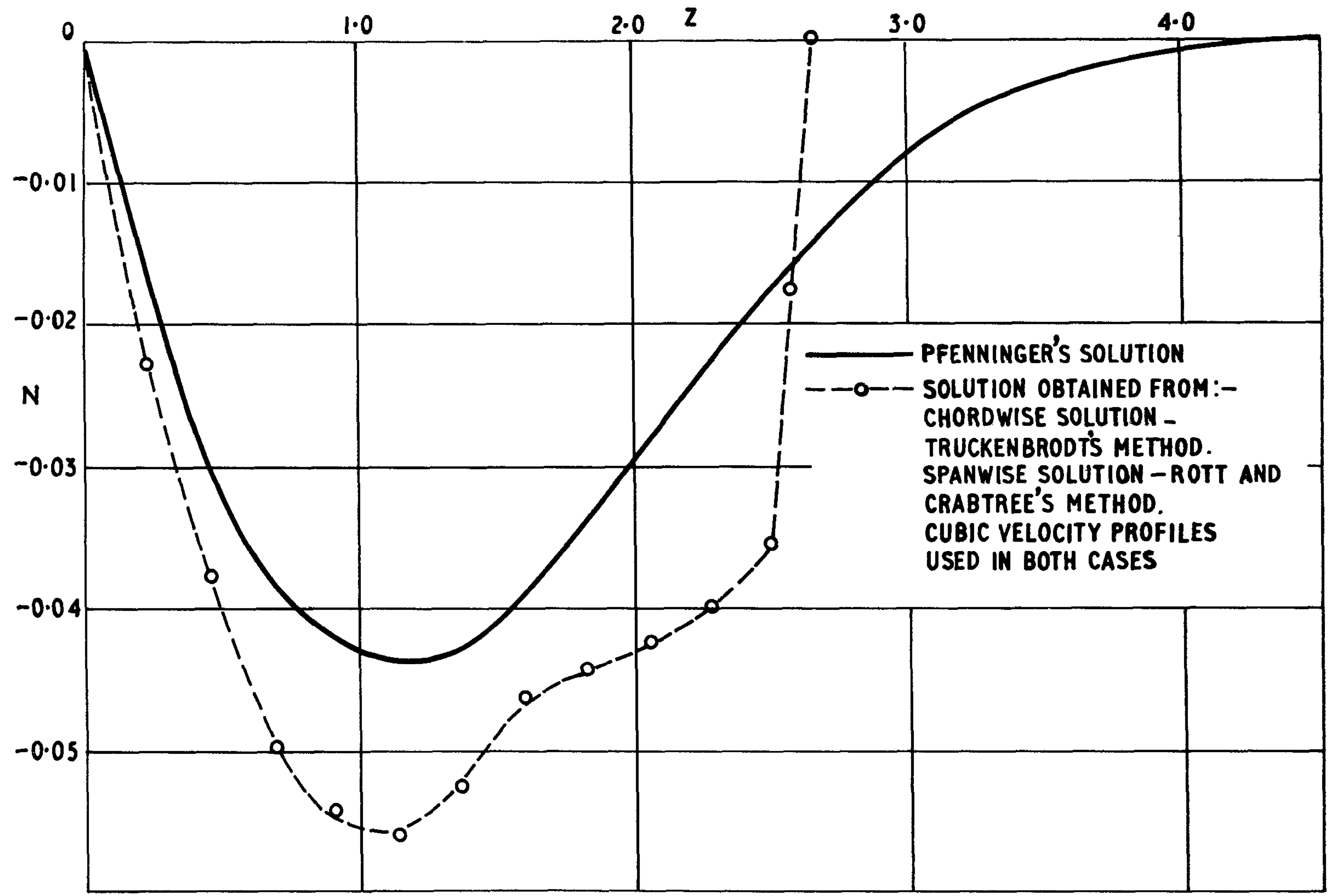

FIG. 3. EARLY ATTEMPT AT PROFILE COMPARISON AT 63% CHORD

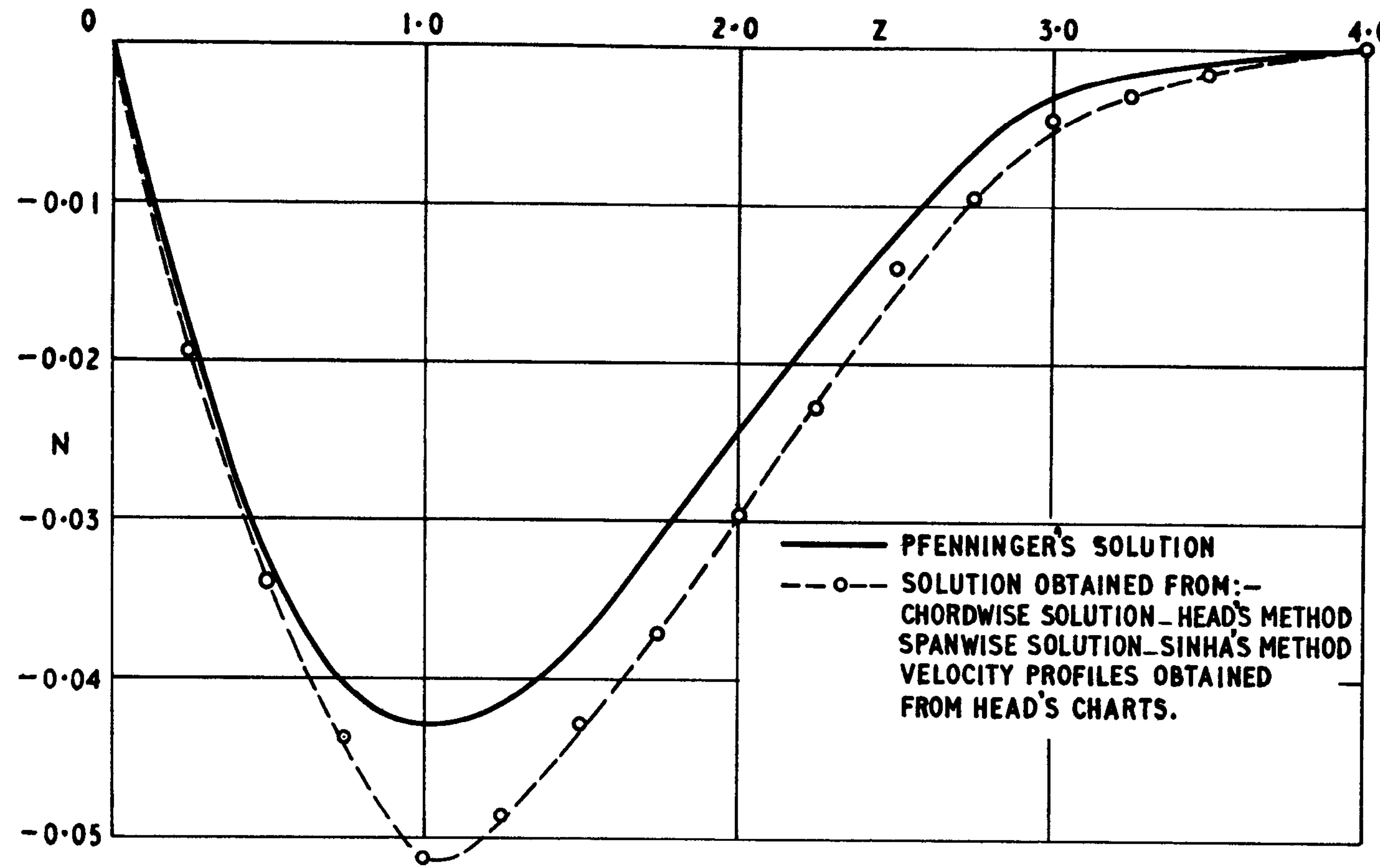

FIG. 4. EARLY ATTEMPT AT PROFILE COMPARISON AT 50% CHORD

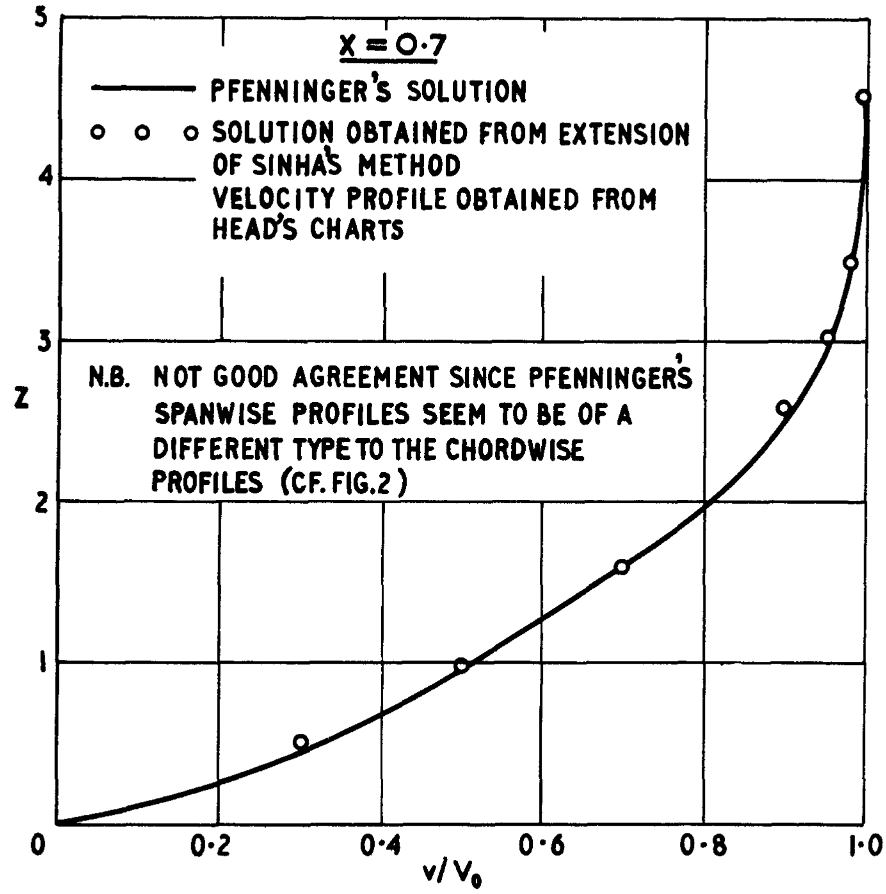

FIG. 5. SPANWISE SOLUTION

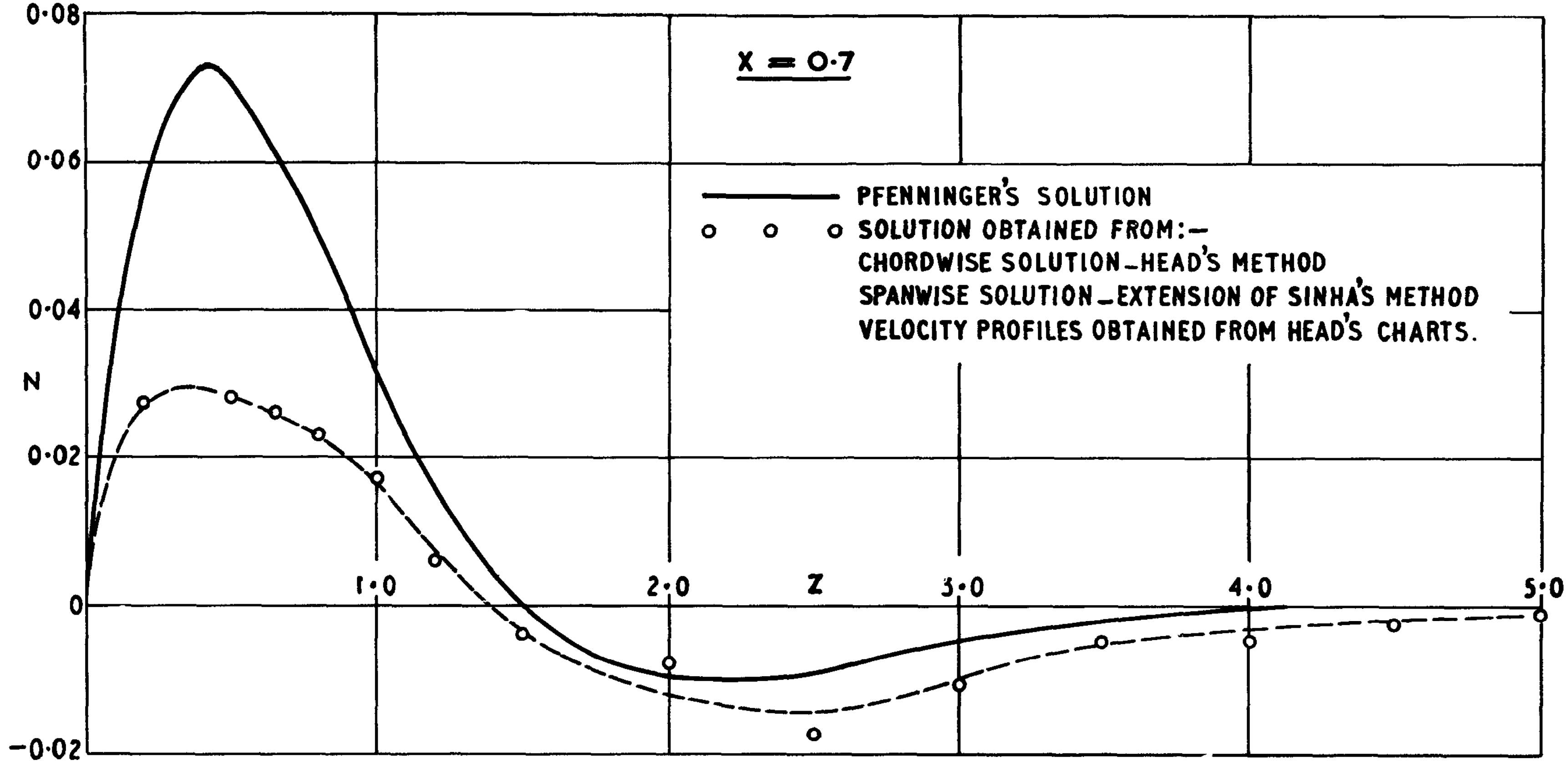

FIG. 6. EARLY ATTEMPT AT PROFILE COMPARISON AT 70% CHORD

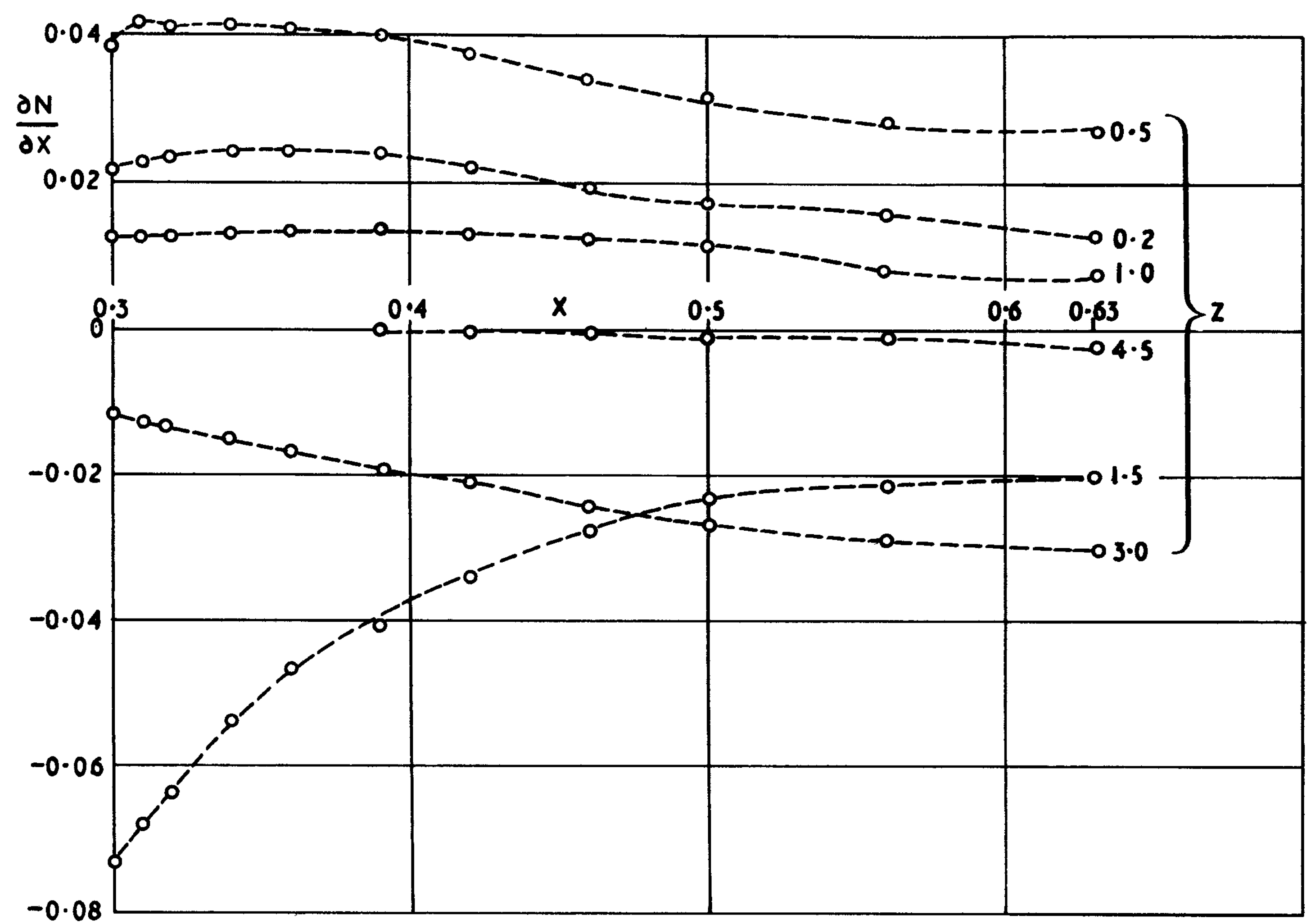

FIG. 7. RUNNING PLOT OF $\frac{\partial N}{\partial X}$ FROM X = 0·3 TO 0·63

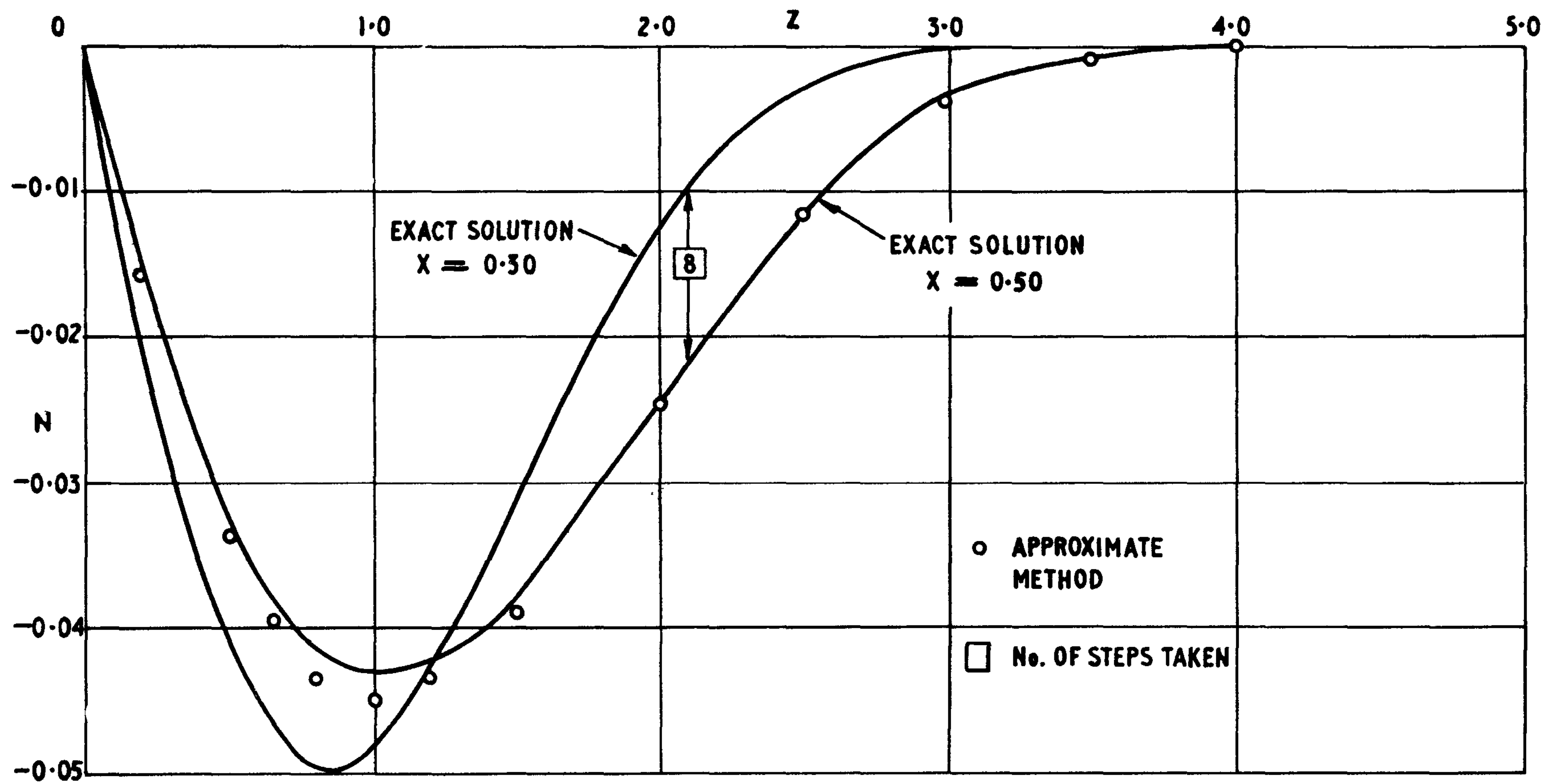

FIG.8. PROFILE COMPARISON AT 50% CHORD

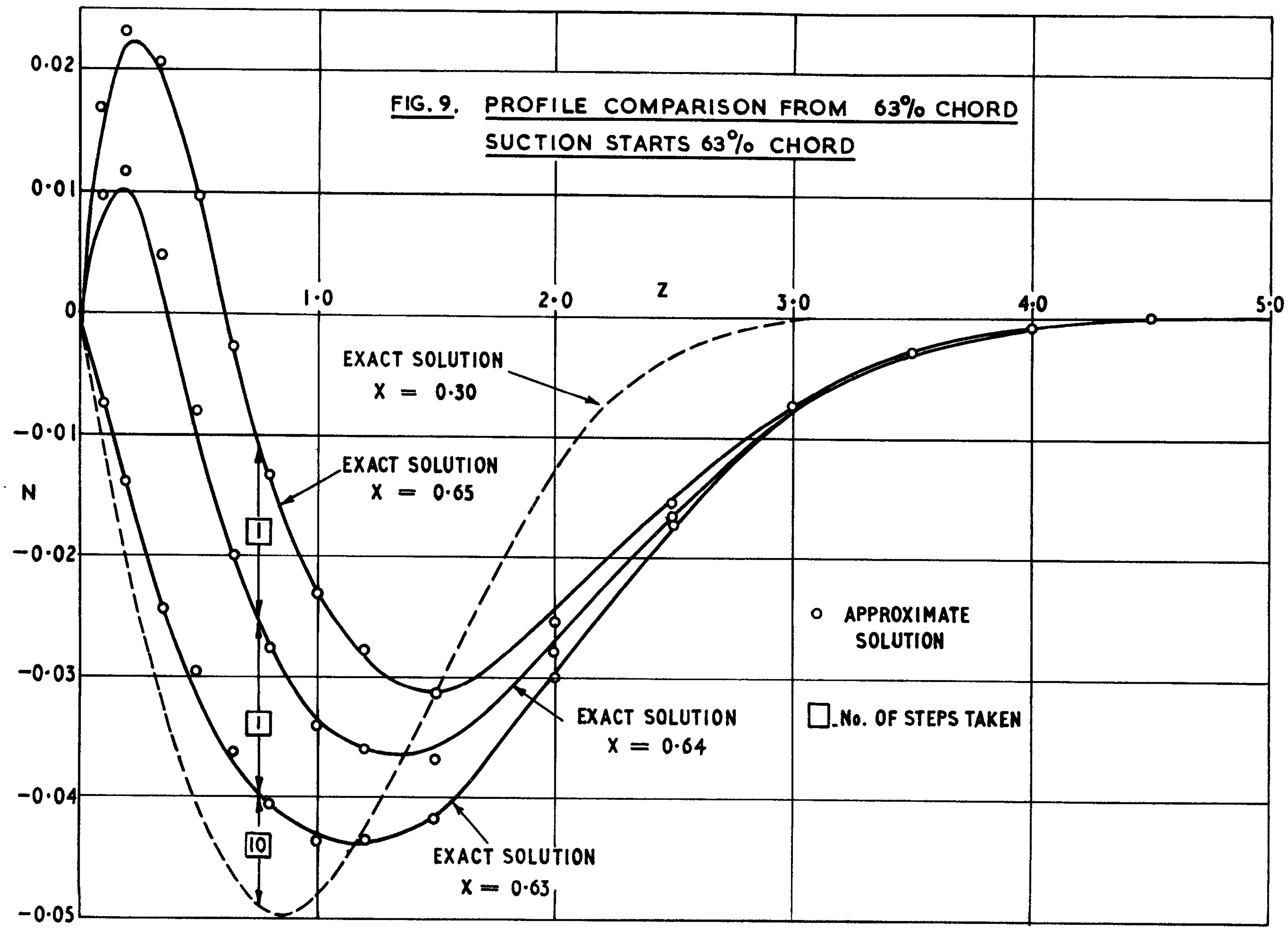

FIG. 9. PROFILE COMPARISON FROM 63% CHORD
SUCTION STARTS 63% CHORD
0·02
0·01
0
−0·01
−0·02
−0·03
−0·04
−0·05
N
Z
1·0
2·0
3·0
4·0
5·0
EXACT SOLUTION X = 0·30
EXACT SOLUTION X = 0·65
EXACT SOLUTION X = 0·64
EXACT SOLUTION X = 0·63
1
1
10
APPROXIMATE SOLUTION
No. OF STEPS TAKEN

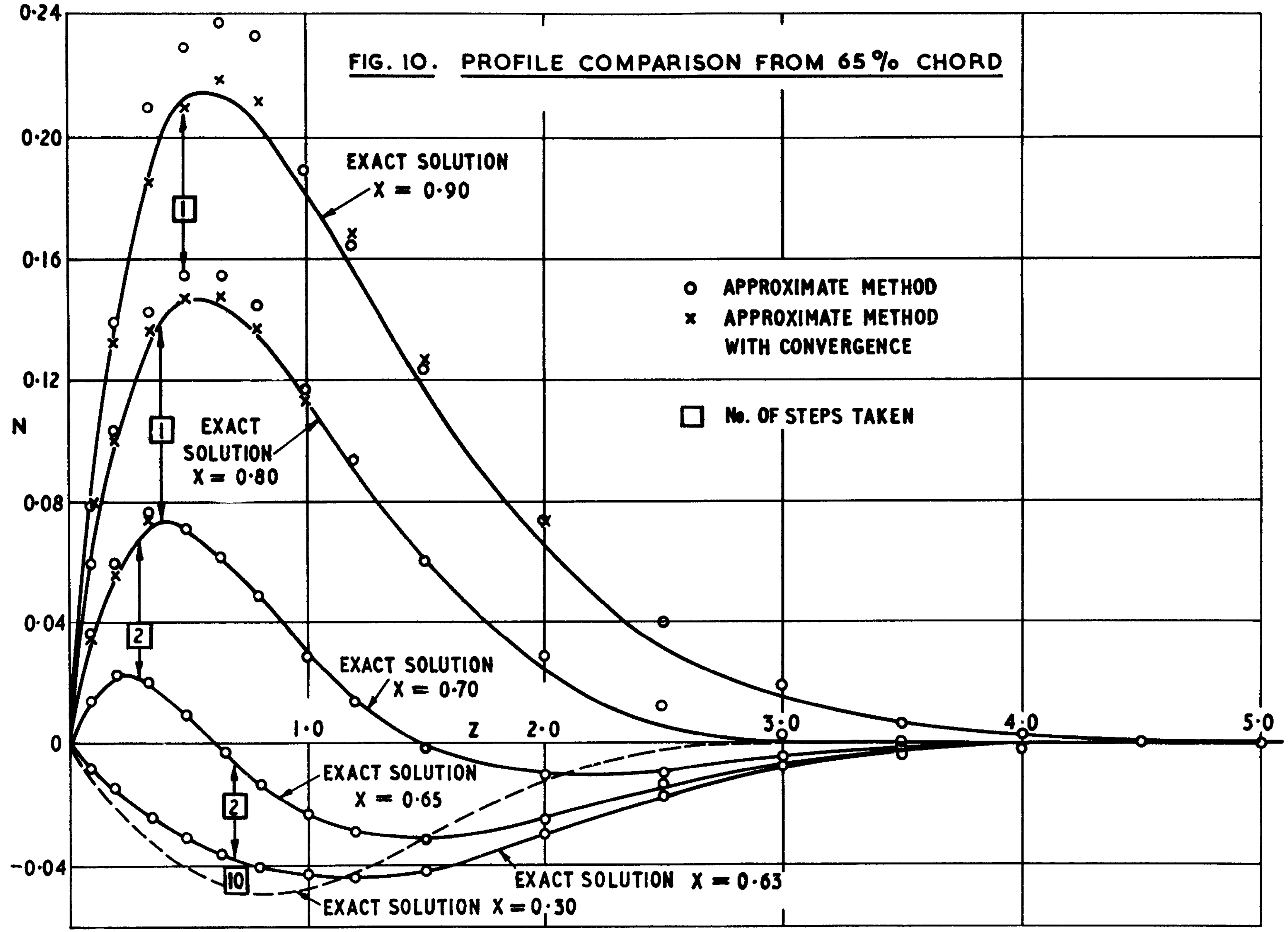

FIG. 10. PROFILE COMPARISON FROM 65% CHORD
0·24
0·20
0·16
0·12
0·08
0·04
0
-0·04
N
1·0
Z
2·0
3·0
4·0
5·0
EXACT SOLUTION X = 0·90
EXACT SOLUTION X = 0·80
EXACT SOLUTION X = 0·70
EXACT SOLUTION X = 0·65
EXACT SOLUTION X = 0·63
EXACT SOLUTION X = 0·30
APPROXIMATE METHOD
APPROXIMATE METHOD WITH CONVERGENCE
No. OF STEPS TAKEN
1
1
2
2
10

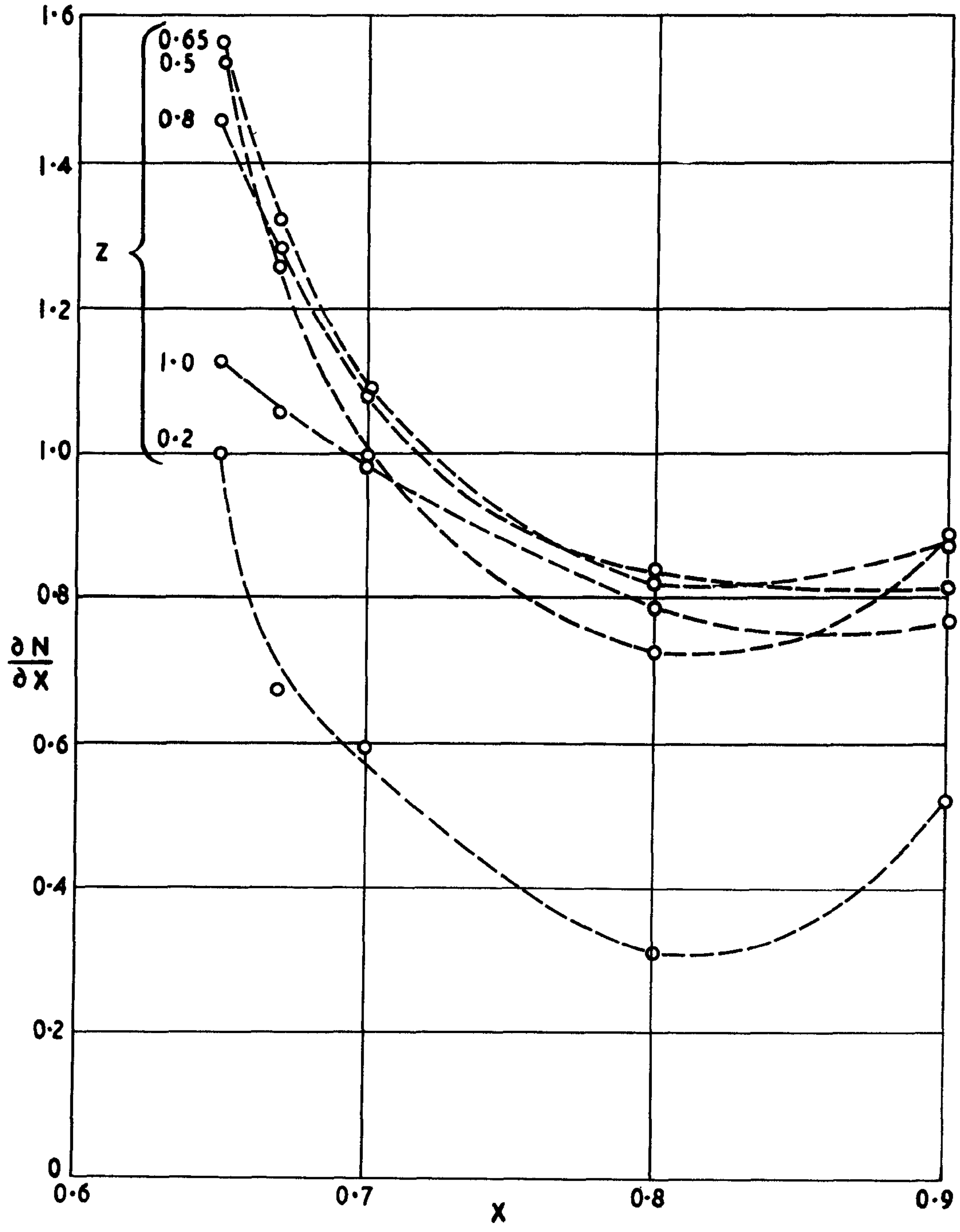

FIG. 11. INITIAL PLOTS OF $\frac{\partial N}{\partial X}$ IN THE SUCTION REGION FOR Z BELOW UNITY

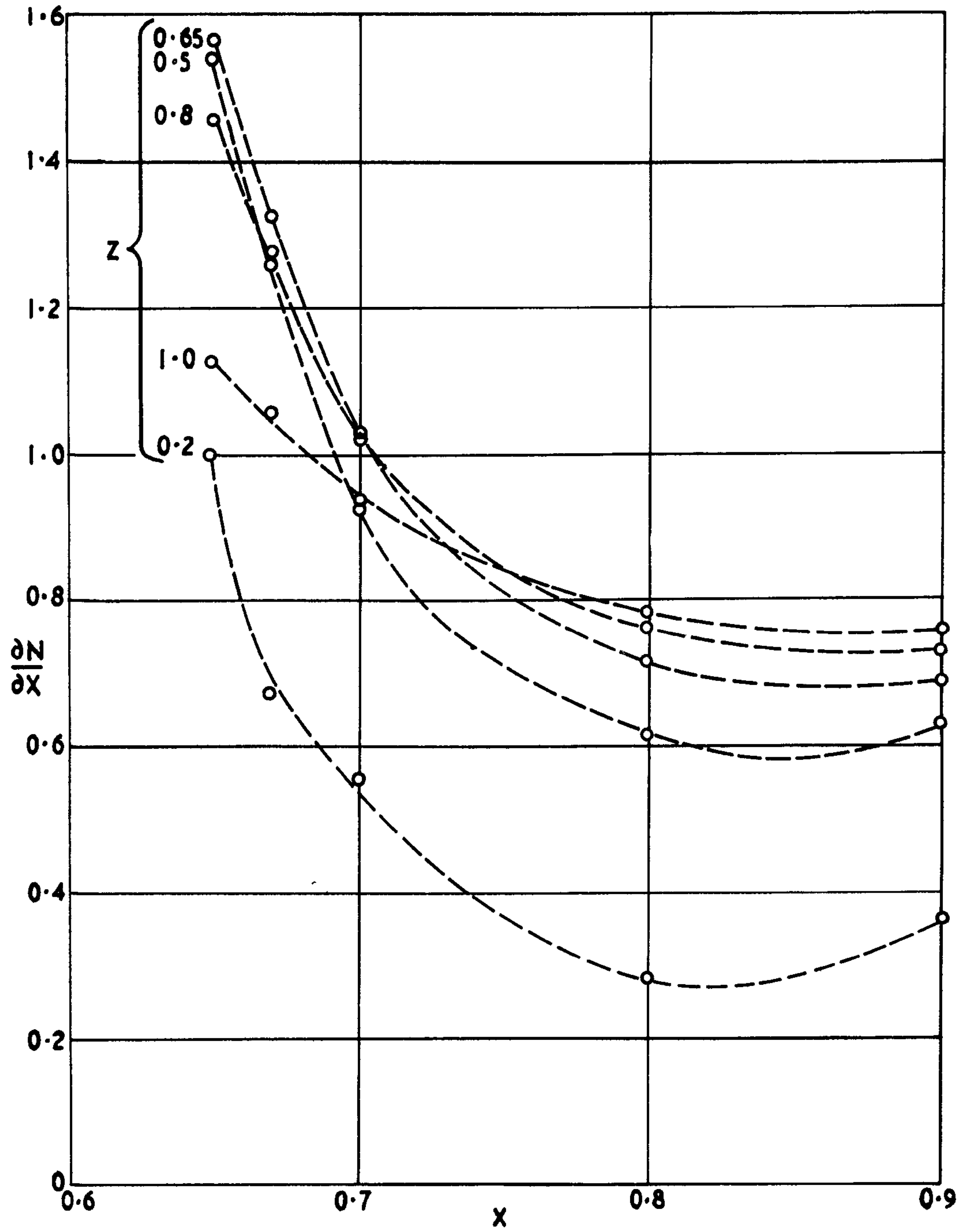

FIG. 12. AS THE PLOTS OF FIG. 11. BUT AFTER AVERAGING THE $\frac{\partial N}{\partial X}$'S AT X=0·7, 0·8 & 0·9

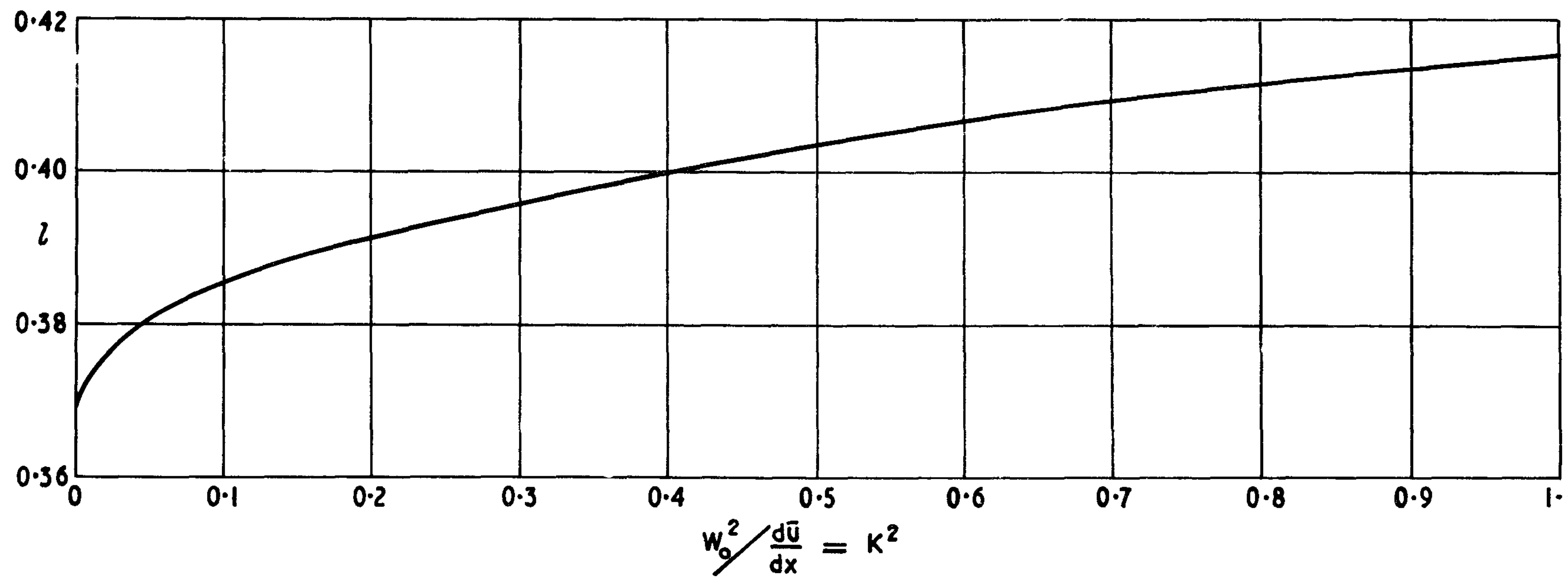

FIG. 13. CHORDWISE STAGNATION VALUE OF l FOR ARBITRARY VELOCITY GRADIENT AND SUCTION

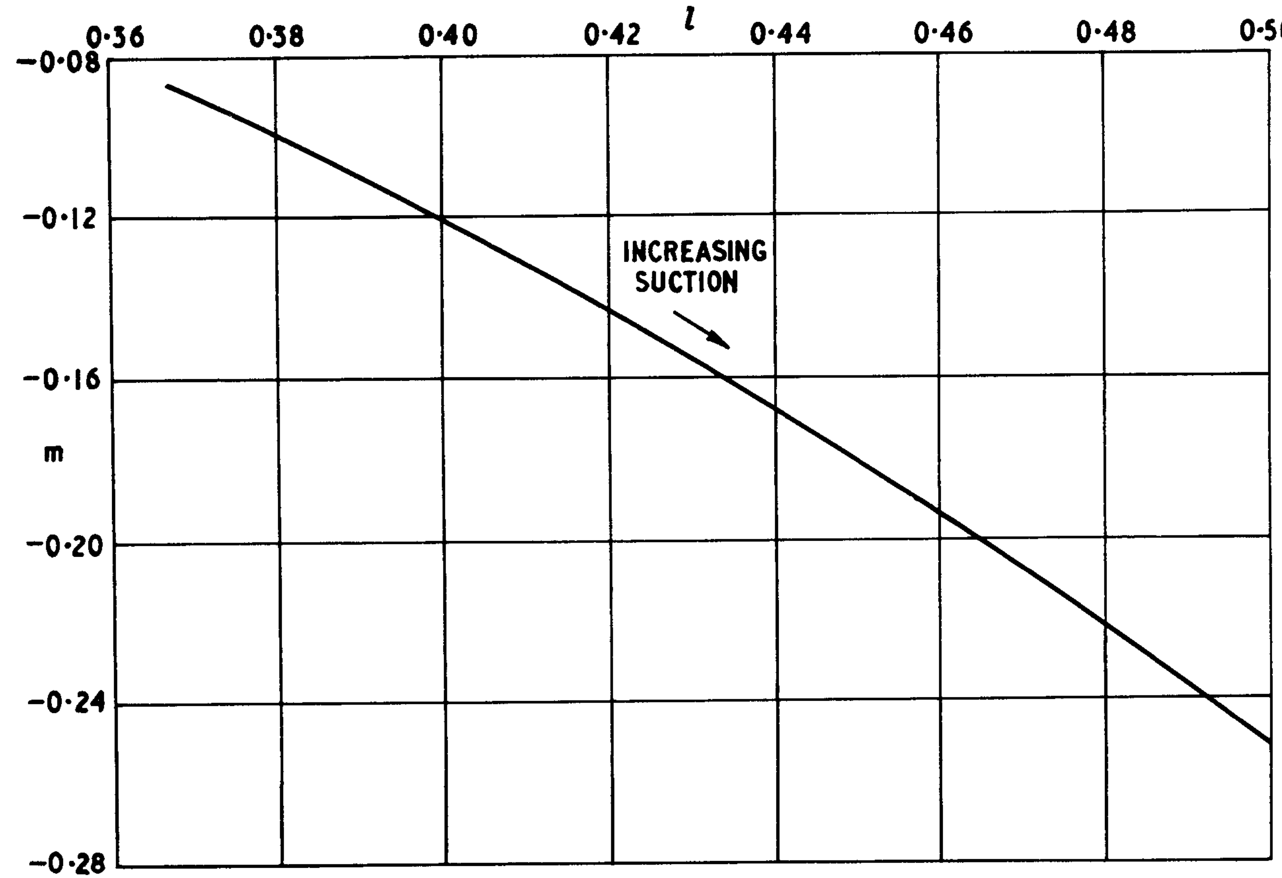

FIG. 14. CHORDWISE STAGNATION VALUES OF l AND m

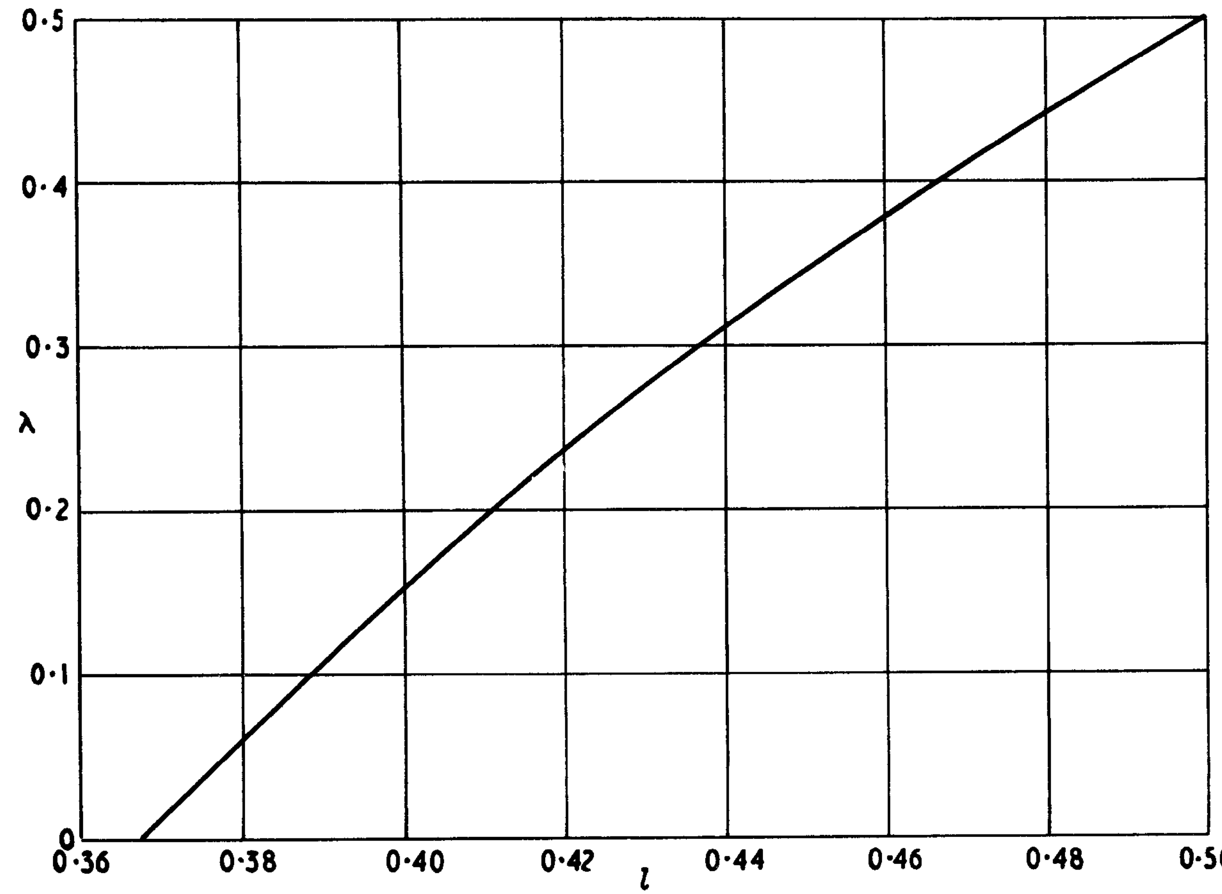

FIG. 15 CHORDWISE STAGNATION VALUE OF λ

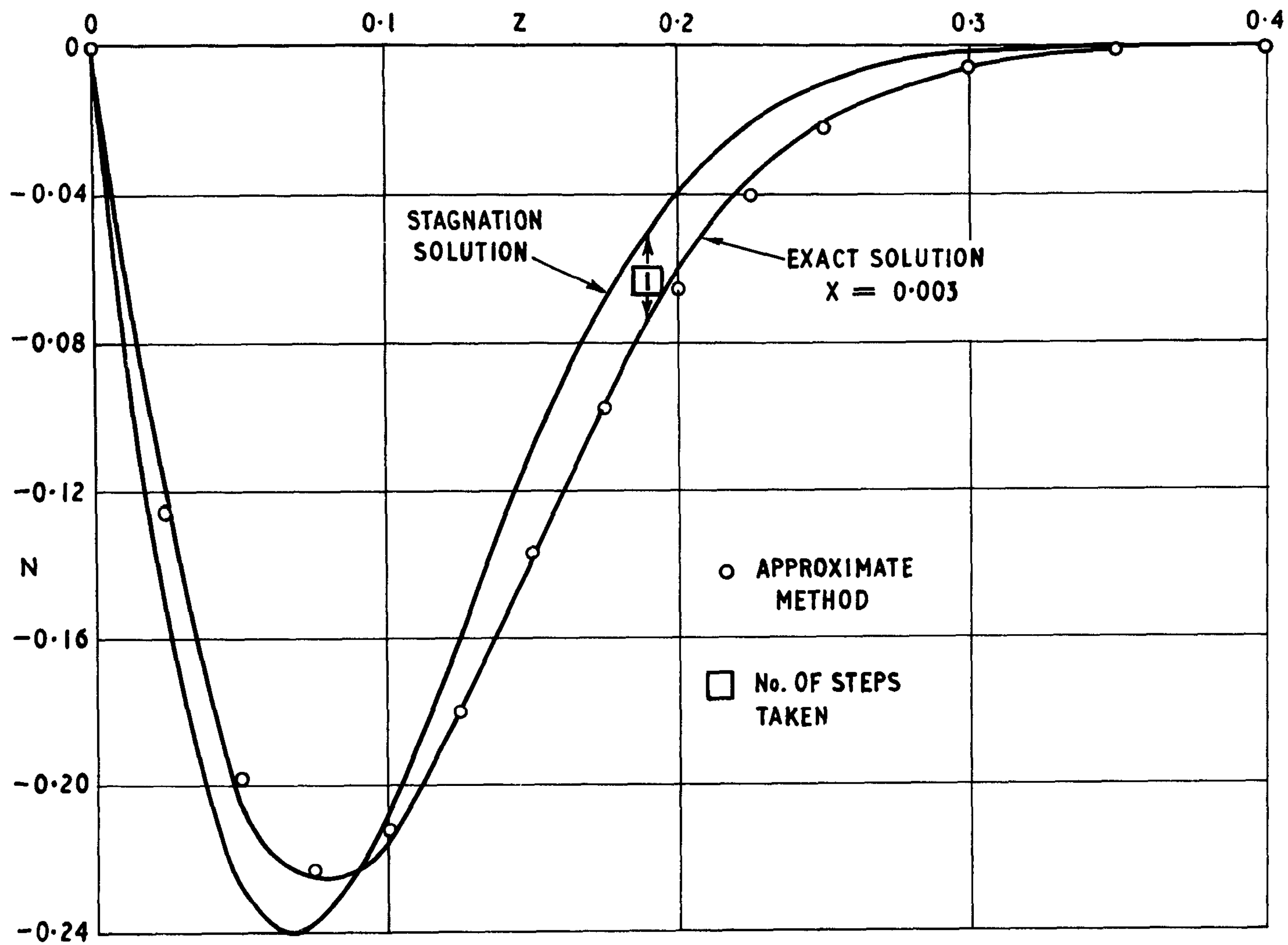

FIG. 16. PROFILE COMPARISON NEAR STAGNATION

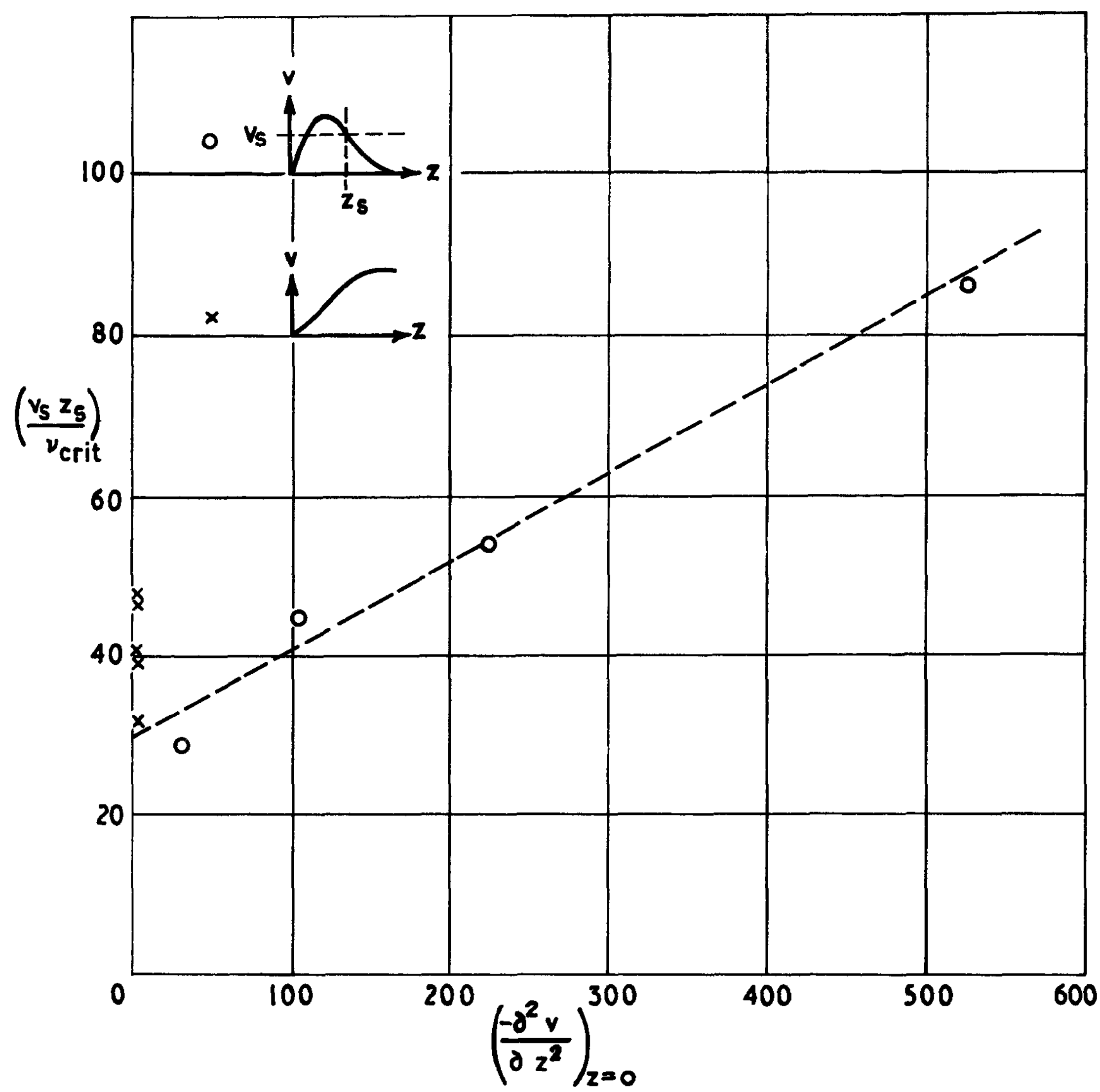

FIG. 17. A CRITERION FOR THE STABILITY OF THE BOUNDARY LAYER WITH INFLEXION POINTS.

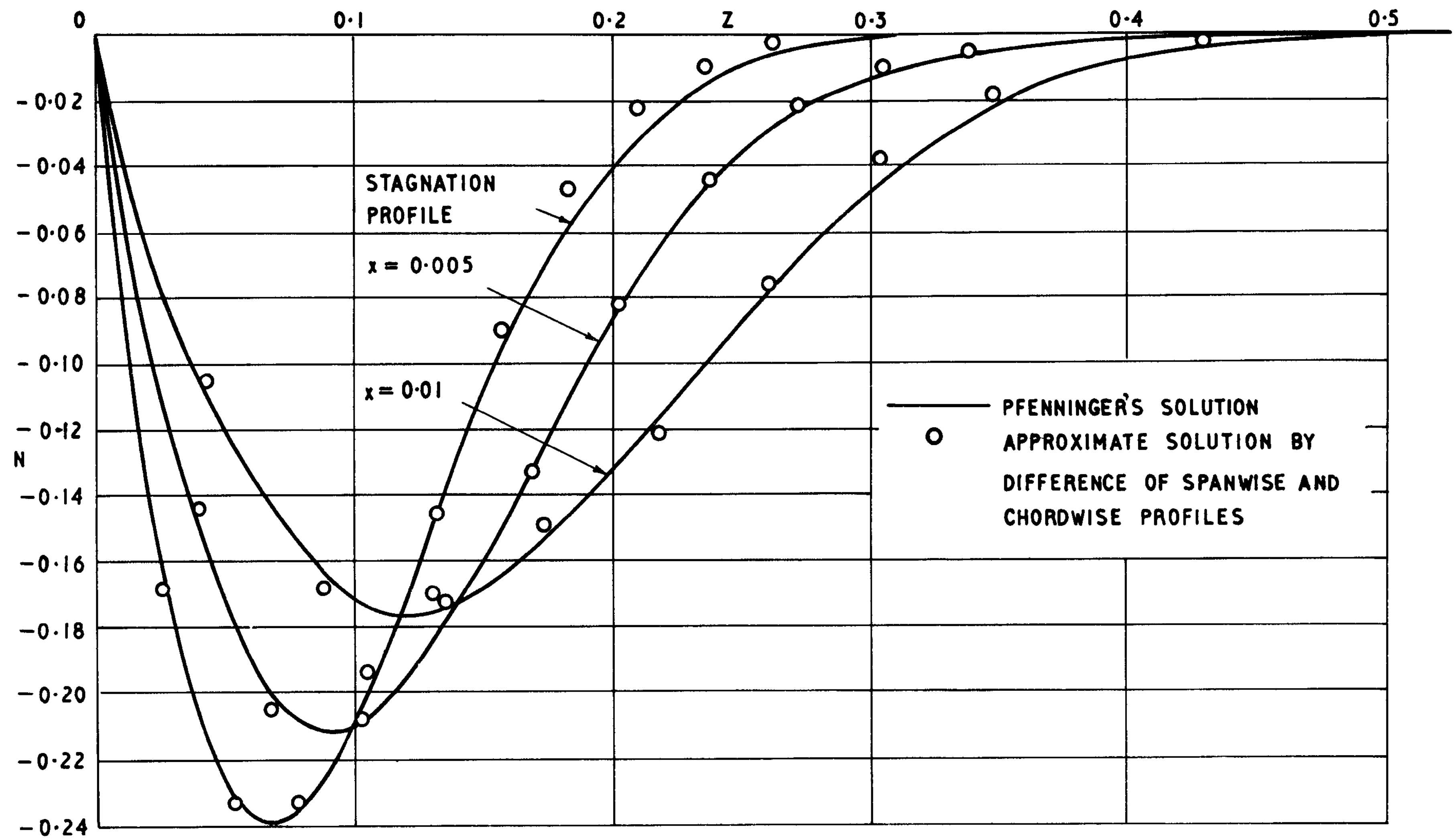

FIG. 18. PROFILE COMPARISON FROM STAGNATION.

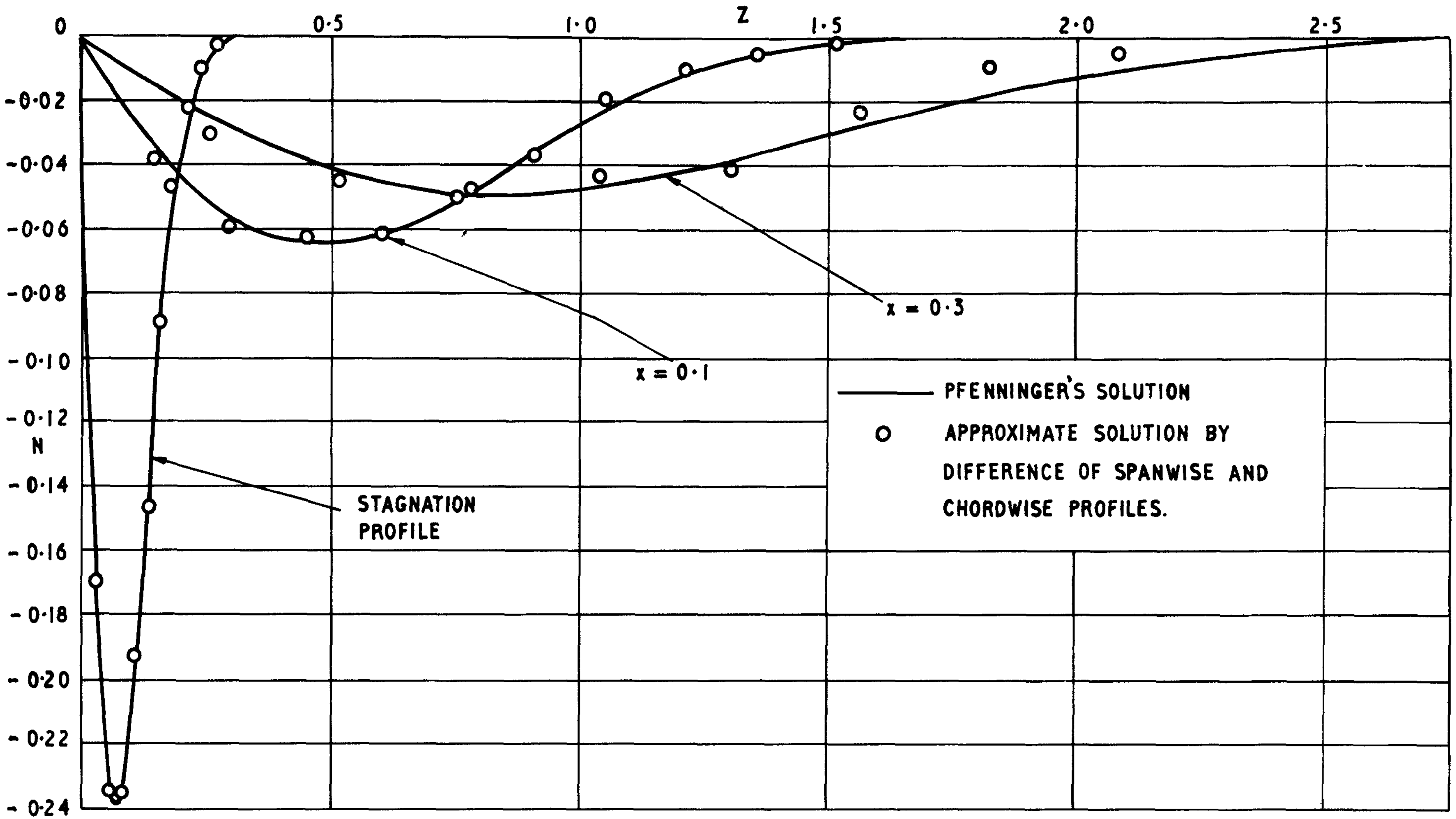

FIG. 19. PROFILE COMPARISON FROM STAGNATION.

C.P. No. 516

(19,522)
A.R.C. Technical Report

Printed and published by
HER MAJESTY'S STATIONERY OFFICE

To be purchased from
York House, Kingsway, London W.C.2
423 Oxford Street, London W.1
13A Castle Street, Edinburgh 2
109 St. Mary Street, Cardiff
39 King Street, Manchester 2
Tower Lane, Bristol 1
2 Edmund Street, Birmingham 3
80 Chichester Street, Belfast 1
or through any bookseller

Printed in England

S.O. Code No. 23-9012-16

C.P. No. 516